(NASA-CR-173196) IMPACT EXPERIMENTS IN VISCOUS FLUID MEDIA Semiannual Status Report for period ending Jan. 1984 (Arizona State Univ.) 83 p HC A05/MF A01 CSCL 08C

N84-16745

Unclas
G3/48 00597

Long period Rayleigh wave and Love wave dispersion data, particularly for oceanic areas, have not been simultaneously satisfied by an isotropic structure. In this paper available phase and group velocity data are inverted by a procedure which includes the effects of transverse anisotropy, anelastic dispersion, sphericity, and gravity. The resulting models, for average Earth, average ocean, and oceanic regions divided according to the age of the ocean floor, are quite different from previous results which ignore the above effects. The models show a low-velocity zone with age dependent anisotropy and velocities higher than derived in previous surface wave studies. The correspondence between the anisotropy variation with age and a physical model based on flow aligned olivine is suggestive. For most of the Earth SH>SV in the vicinity of the low-velocity zone. Near the East Pacific Rise, however, SV>SH at depth, consistent with ascending flow. Anisotropy is as important as temperature in causing radial and lateral variations in velocity. The models have a high velocity nearly isotropic layer at the top of the mantle that thickens with age. This layer defines the LID, or seismic lithosphere. In the Pacific, the LID thickens with age to a maximum thickness of about 50 km. This thickness is comparable to the thickness of the elastic lithosphere. The LID thickness is thinner than derived using isotropic or pseudo-isotropic procedures A new model for Average Earth is obtained which includes a thin LID. This model extends the fit of a P.R.E.M. type model to shorter period surface waves.

INTRODUCTION

Rayleigh wave and Love wave phase and group velocity data have been collected and inverted for upper-mantle structure by many authors. Some of the more recent studies are Schlue and Knopoff [1977; 1978], Mitchell and Yu [1980], Silver and Jordan [1981], Forsyth [1975a; 1975b], Dziewonski and Anderson [1981] , Mills and Hales [1977], Wielandt and Knopoff [1982], Nakanishi and Anderson [1982], Anderson and Hart [1976], Nakanishi [1981], Anderson [1982; 1983], and Montagner and Jobert [1983]. Many studies have derived regional phase and/or group velocities for several regions believed to be physically different. For example, the earth can be divided into oceanic, tectonic, and continental regions [Toksoz and Anderson, 1966; Nakanishi and Anderson, 1983; Mills and Hales, 1978b; Dziewonski and Steim, 1982; Silver and Jordan, 1981] or the ocean can be divided on the basis of the age of the seafloor [Forsyth, 1975a; 1975b; Mitchell and Yu, 1980; Montagner and Jobert, 1983; Schlue and Knopoff, 1977; 1978]. However, the data derived in these studies have not been inverted using a procedure that accounts completely and directly for the effects of anisotropy, as well as sphericity, gravity and anelasticity of the Earth. In this study an average Earth data-set, an average ocean data-set, and a data-set for a number of regionalized ocean age provinces will be modeled using a procedure that includes anisotropy, sphericity, gravity, and anelasticity. The data sets were collected from the literature.

The regionalized oceanic data have been used to derive models of the variation with depth of SH velocity, using Love wave velocity data, and the variation with depth of SV velocity, from Rayleigh wave data. These models have been used to investigate how the velocity and the thickness of the oceanic lithosphere and the velocity in the low velocity zone (LVZ) vary with age. Forsyth [1975a] concluded that Rayleigh waves travel fastest in the direction of spreading and

that Love wave and Rayleigh wave data were inconsistent unless SH> SV in at least the upper 125 km. He also believed that anisotropy might be present below 250 km. Schlue and Knopoff [1977] found that the LVZ was anisotropic but the crust and lid could be modeled as isotropic. Their LVZ extends from 180 km to the bottom of the lid (15 km - 115 km depending on age). They comment that the observed P_n velocity can be explained by a thin sub-moho layer that would not be resolved by their data. Schlue and Knopoff [1978] included anisotropy in the LVZ for a suite of calculated models. Yu and Mitchell [1979] and Mitchell and Yu [1980] find anisotropy predominantly in the lithosphere and possibly in the LVZ. These studies have found that lithosphere thickness and lithosphere velocity generally increase with age, except Schlue and Knopoff [1977] who constrained their velocities to remain constant with age. The differences in the depth where anisotropy is located in these studies can be attributed to differences in the assumptions, the constraints, the inversion methods, or to some systematic.

The most serious source of systematic error is the separate isotropic inversion of Love and Rayleigh waves to give an anisotropic structure. The studies discussed above are almost all based on pseudo-isotropic inversions that determine SV velocity from isotropic Rayleigh wave inversion and SH velocity from isotropic Love wave inversion. The differences between the two models are then used as a measure of the anisotropy. Separate isotropic inversions make no allowance for P-wave anisotropy, and include neither the effects of SV velocity on Love wave velocities nor the effect of changes in PV, PH, and SH velocities on Rayleigh waves. Thus, the procedure of using separate isotropic inversions is useful only to indicate the probable presence of anisotropy, or to calculate responses for propagation in planes perpendicular to the symmetry axis in a transversely isotropic medium [Crampin, 1970]. Some studies [Yu and Mitchell,

1979; Montagner and Jobert, 1983] cite a statement made by Crampin and King [1977] that for low resolution data of an anisotropic earth an isotropic inversion is valid. Of course, the resulting model is necessarily of equally low resolution, and only the gross properties of the model may be believed. Thus the pseudo-isotropic inversion procedure is self limiting. No improvement in the amount or quality of the data will improve the quality of the model since the procedure itself becomes invalid when the resolution improves. Anderson [1966], Dziewonski and Anderson [1981], and Anderson and Dziewonski [1982] have shown that in the presence of anisotropy important errors are introduced by using a pseudo-isotropic procedure. Kirkwood [1978] also shows the necessity for the inclusion of anisotropy in the inversion. Thus, a complete anisotropic inversion would be useful and could produce different results than a pseudo-isotropic approach. An anisotropic inversion would have the advantage that no error would be introduced by the incorrect pseudo-isotropic procedure, allowing increased resolution in the presence of enough data.

The inclusion of anisotropy introduces new difficulties to the problem. For the case of transverse anisotropy considered here the number of free parameters in each layer increases from three (density, P velocity, S velocity) to six (density, horizontal and vertical P velocities, horizontal and vertical S velocities, and a velocity in some intermediate direction). The resolving power of the fundamental mode surface wave data used here are insufficient to determine all of the parameters in models with even the simplest forms of parameterization. To overcome this problem additional constraints must be applied. The particular constraints used in this paper will be discussed later.

As illustrated by the differences between the results of previous studies the parameterization, the class of models, and the constraints applied can have a significant effect on the final models even for an isotropic inversion. While each

of the studies was self-consistent and according to the appropriate set of resolving kernels gave a good indication of the type and location of anisotropy, the depth and extent of anisotropy was different for each study. While the difference in anisotropy may be partially caused by the pseudo-isotropic procedure the differences between individual isotropic SV or SH models is also large. If one attributes those differences to changes in model type, parameterization, and constraints between studies, it is reasonable to expect that a full anisotropic parameterization, with its increased number of parameters, might yield different results. The increased number of parameters available vastly increases the number of possible models that will fit the data within a given range of uncertainty. The problem of non-uniqueness becomes even more pronounced. The final models are dependent on the parameterization and the assumptions. The models derived in this study are a possible set of anisotropic models that agree with the fundamental mode Rayleigh wave and Love wave data for periods less than 300 seconds. They can be used to illustrate how large a difference the introduction of anisotropy can make to models of the velocity structure of the upper mantle.

DATA

The data used in this study were compiled from many sources discussed in detail below. Data sets were collected for the average Earth, the average ocean, and for several regions of the Pacific divided according to the age of the ocean floor. Each data set consisted of phase and/or group velocities of Rayleigh and/or Love waves. For the average Earth, the average ocean, and the regionalized provinces 0-10, 0-20, 20-50, 50-100, and >100 M.Y. in age all four types of data were available. For the regionalized provinces 0-5, 5-10, and 10-20 M.Y. in age only Rayleigh wave data were available.

The data for the average Earth are given in tables 1 and 2 and shown, along with the corresponding models, in figures 1 and 2. A large set of fundamental mode data was compiled from the sources discussed below. Nakanishi and Anderson [1983a; 1983b] give group velocities for Love and Rayleigh waves between 100 seconds and 400 seconds period and phase velocities between 100 and 300 seconds period. Phase and group velocity values were determined from about 200 paths using the single station method or great-circle measurements. Spherically averaged velocities given here are part of the results of an inversion to give a spherical harmonic representation of the variations in great-circle velocity. Fukao and Kobayashi [1983] also give data of all four types for periods between 100 and 400 seconds. These data are the averages, and the quoted uncertainties are the standard deviations of the velocities resulting from using a time variable filtering technique on data from 37 great-circle paths from the 1963 Kurile islands earthquake. All fundamental mode data from these sources are included in the data set. Dziewonski and Steim [1982] give spheroidal mode periods and Rayleigh group velocities for ${}_0S_9$ to ${}_0S_{55}$ that correspond to periods of 165 to 640 seconds. Selected modes for the period range 160 to 400 seconds are given in table 1. The modes chosen are ${}_0S_{17}$ to ${}_0S_{25}$, every second mode, and ${}_0S_{25}$ to ${}_0S_{55}$, every third mode. The intermediate modes are, for the most part, consistent with the other data and form a reasonably smooth curve with the modes used. Therefore, the included modes are a good indication of the quality of the fit of the model to the part of this data set with periods less than 400s. This data set was derived from 37 seismograms from several sources by using a waveform inversion technique to determine dispersion curves for each source-receiver pair. Then a pure path analysis was conducted to give group velocities and normal mode periods. Mills and Hales [1978a] give Rayleigh group velocities for periods of 50 to 300s, and normal mode periods for ${}_0S_{25}$ to ${}_0S_{195}$. Rayleigh

group velocity values for periods between 50 and 300 seconds and phase velocities derived from the normal mode periods of selected modes are given in table 2. The uncertainties in the group velocity portion of their data set varied by an order of magnitude between two tables containing some of the same data. The uncertainties in Mills and Hales [1977] were taken as correct. The uncertainties quoted in Mills and Hales [1978a] were corrected to conform with Mills and Hales [1977]. These group velocities were derived by averaging a set of path averaged great-circle group velocity estimates based on seismograms from several large events in the Kurile Islands. The phase velocities were determined by integrating the group velocities. The data discussed above, although derived by different methods, are, in almost all, cases consistent between data sets to within quoted uncertainties.

The data for the average ocean are given in tables 3 to 6, and shown in figures 3 and 4. Mitchell and Yu [1980] give data for four regionalized oceanic provinces. The data are derived from a pure path analysis of single station measurements for 33 Rayleigh and 30 Love wave paths in the Pacific that are predominantly oceanic. To approximate average ocean the Rayleigh and Love group and phase velocity data for the two intermediate age provinces, 20-50 M.Y. and 50-100 M.Y., were averaged. This provides oceanic data for periods between 20 and 110 seconds. Kanamori [1970] gives average oceanic Love and Rayleigh wave phase velocities between 125 and 300 seconds resulting from a pure path analysis of 25 great-circle phase velocity measurements. Mills and Hales [1978b] give oceanic Rayleigh wave group velocities between 50 and 540 seconds. All average ocean data from these sources for periods less than 300 seconds are given in tables 3-6, and shown in figure 3 and 4. Dziewonski and Steim [1982] give oceanic Rayleigh wave group velocities and normal mode periods for average ocean for periods between 165 and 635 seconds. These data were derived

using the analysis described in the average Earth section. The same modes used for the average earth data set are used for this data set. As for the average Earth data set, the remaining modes form a smooth curve with the modes used. Therefore, the modes used are a good indication of the quality of the fit to the model of the data set for periods less than 300 seconds. The collected data from the above sources are generally consistent with each other within the quoted uncertainties.

The data for regionalized oceanic provinces, predominantly from Mitchell and Yu [1980] and Forsyth [1975a; 1975b], are shown along with best fitting models in figures 5 to 8 and listed in tables 7 to 15. The regionalization of Mitchell and Yu [1980] consists of four provinces with age ranges 0-20 M.Y., 20-50 M.Y., 50-100 M.Y., and >100 M.Y. For each of these regions short period data of all four types are given. Some of the regions of Forsyth [1975a, 1975b] were also used. These four regions are 0-5 M.Y., 5-10 M.Y., 10-20 M.Y., and 0-10 M.Y. The former data are derived from a pure path analysis of measurements in the entire Pacific basin while the latter data are derived from a similar study using measurements in the Nazca plate alone. For the 0-20 M.Y old region the East Pacific Rise Rayleigh phase velocity data of Wielandt and Knopoff [1982] for periods of 40-300 seconds were added to the corresponding Mitchell and Yu [1980] data set that covers a period range of 20 to 102 seconds. The latter data set is consistently slower by 0.005 to 0.02 km/s. The difference increases as the period becomes shorter. The differences are within quoted uncertainties of the data. Forsyth's >20 M.Y. old province is equivalent in age to the 20-50 M.Y. old province of Mitchell and Yu [1980]. Combining the two sets of Rayleigh wave phase and group velocity data shows that in general Forsyth's data are about 0.005-0.01 km/s faster. Again the differences are well within quoted uncertainties. The data sets for 50-100 M.Y. old ocean are entirely from Mitchell and Yu

[1980] and contain all four types of data. The data sets for >100 M.Y. old ocean contained only Mitchell and Yu's data when the models were determined. However, the Rayleigh phase velocity data of Souriau and Souriau [1983] were added after the model was derived. These data, which fit the model already calculated to within two standard deviations, are based on a pure path analysis using the combined velocity data of Kanamori [1970], Dziewonski [1970], Wu [1972], Dziewonski and Gilbert [1972], Okal [1977], Nakanishi [1979], and Leveque [1980]. Rayleigh wave data sets for the remaining provinces, 0-5 M.Y., 5-10 M.Y., 10-20 M.Y., and 0-10 M.Y., are from Forsyth (1975a). Love wave data from Forsyth (1975b) are given for the 0-10 M.Y. old province. New Rayleigh wave group velocity data from Montagner and Jobert [1983] were compared with the models, and generally agree with these except in the 50-100 M.Y. old province. However ,these data cover an increased period range of 40-300 seconds and thus would expand the data coverage.

STARTING MODELS

The introduction of anisotropy increases the number of free parameters in any inversion of the data and thus makes the choice of starting model and/or reference model more critical to the final model. The model parameterization and constraints need to be chosen to reduce the number of parameters the data will be required to resolve to a reasonable level. In each layer of a transversely isotropic model five elastic parameters, density, and a Q value, are needed to calculate a response. The elastic parameters can be in terms of the elastic constants, A, C, N, L, and F [Love, 1927] or in terms of wave velocities. The latter parameters were used for P.R.E.M. [Dziewonski and Anderson, 1981] and will be used here. Thus, the elastic parameters are VSV, VPV (vertical S-wave and P-wave velocity respectively), VSH, VPH (horizontal SH and P velocity respectively), and ETA. ETA determines how the P velocity and S velocity vary at

intermediate angles of incidence and can be expressed as follows:

$$ETA = \frac{F}{A - 2L}$$

To make comparison of the models to P.R.E.M. easier the structure of the P.R.E.M. model was used for this study. The models, therefore, consist of an ocean layer, an upper and lower crust, a region above the LVZ (the LID), a LVZ, and a region between the bottom of the LVZ (220 km) and 400 km. Below 400 km all models are identical to P.R.E.M. As in the P.R.E.M. model anisotropy was introduced only between the base of the crust and the bottom of the LVZ; all other regions in the model are isotropic. The Q model from P.R.E.M. was used in all cases. The number of layers for which parameters must be determined was minimized by using a P.R.E.M. like polynomial representation. In the upper 400 km, where parameters were allowed to vary in this study, each region (LID, LVZ, etc) can be treated as a single unit with a mean value and a linear gradient for each of the velocities, density, and ETA. Below 400 km P.R.E.M. has several regions described by linear, quadratic and cubic polynomials. These layers are not changed in any model discussed in this paper. Thus, the form of all models in this study can be described as follows:

(1): A water layer, a sediment layer, an upper crustal layer, and a lower crustal layer, all isotropic with constant velocities

(2): A LID whose thickness is allowed to vary at the expense of the LVZ. The LID has a thin (~6 km) upper layer with constant anisotropic velocities consistent with P_n observations. The remainder of the thickness of the LID is a layer of constant isotropic or anisotropic velocities and ETA.

(3): A LVZ whose thickness decreases as the LID thickness increases. The LVZ is a layer where the means and linear gradients of ETA and the four velocity parameters define the structure.

(4): A region between 220 and 400 kilometers where the linear gradients and means of ETA and the four velocity parameters define the structure.

(5): The density and Q in each region are the same as in P.R.E.M. The means of the four velocities and ETA in all regions and gradients of velocities and ETA in regions 3 and 4 vary between models.

(6): Below 400 kilometers the models are all identical to P.R.E.M.

The starting models used were all similar to P.R.E.M. but were different for each data set. Some features were common to many data sets. For example, the water and sediment depths for all the regional data sets were derived from those of Leeds, Knopoff, and Kausel [1974]. A six kilometer thick upper lid layer with velocities consistent with P_n and S_n data was inserted below the crust for each of these regions, for the average Earth, and for the average ocean. Below 400 km all models were identical to P.R.E.M. Above 400 km, density and Q in each depth interval were the same as in P.R.E.M. Differences in the starting models are discussed in the remainder of this section.

For the average Earth data set P.R.E.M. itself was the starting model. For the average ocean the starting model consisted of P.R.E.M. below 40.8 km, a 30 km LID with VPV=VPH=8.214 km/s and VSV=VSH=4.600 km/s and ETA=1.0, and the starting model of Yu and Mitchell [1979] for the crust sediment and water layers.

For the regionalization of Mitchell and Yu [1980] starting models were also similar to P.R.E.M. For 0-20 M.Y. old ocean a 3.45 km water layer and a 0.05 km sediment layer were placed on the same crustal starting model as the average ocean data. A 14 km thick lower lid layer with VSV=VSH=4.6 km/s and

VPV=VPH=8.2 km/s was inserted and the LVZ velocities were reduced by 3.5% with respect to P.R.E.M. For the 20-50 M.Y. old ocean a 4.4 km water layer and a 0.1 km sediment layer were placed over the same crust, a 19 km lower lid layer with VSV=VSH=4.68 km/s and VPV=VPH=8.35 km/s, and a LVZ with velocities reduced 2.7% with respect to P.R.E.M. For the 50-100 M.Y. old ocean a water layer of 4.7 km and a sediment layer of 0.3 km as given by Yu and Mitchell [1979] were used. Later, the water layer thickness was adjusted to 5.4 km and the sediment to 0.23 km in a modified starting model consistent with Leeds, Knopoff and Kausel [1974]. A 34 km thick lower lid with VSV=VSH=4.8 km/s and VPV=VPH=8.57 km/s, a LVZ with velocities decreased by 2.25% with respect to P.R.E.M., and a region between 220-400 km were velocities increased by 1% were used. For ocean >100 M.Y. in age a water layer 5.75 km thick, a sediment layer 0.3 km thick, a lower lid 39 km thick with VSH=VSV=4.75 km/s, and a LVZ with velocities increased by 1% and ETA increased by 1.2% with respect to P.R.E.M.

For Forsyth's regions the final model for the 0-20 M.Y. old ocean (table 16) with minor change was used as a starting model. The lid thickness was set to 9 km for 0-5 M.Y., 17 km for 5-10 M.Y., 14 km for 10-20 M.Y. and 0-10 M.Y. The water depth was set to 3.3 km for 0-5 M.Y., 3.5 km for 5-10 M.Y., 3.8 km for 10-20 M.Y., and 4 km for 0-10 M.Y.. No sediment layer was included except for 10-20 M.Y. where 0.02 km of sediment was added.

PROCEDURE

The velocity depth models discussed in later sections were determined by iterative forward modeling. The procedure used to calculate the dispersion curves treats transverse anisotropy in a spherical, anelastic, self gravitating Earth [Takeuchi and Saito, 1972; Dziewonski and Anderson, 1981]. Periods of spheroidal and torsional modes of free oscillation are determined for the given structure. The phase velocities for Rayleigh and Love waves are then calculated

from

$$C = \frac{2\pi R_E}{T \times (n + \frac{1}{2})}$$

where T is the period, n is the mode number, ${}_0S_n$ or ${}_0T_n$, and R_E is the radius of the earth. For all calculations we use R_E = 6371 km.

Modes were chosen to minimize computation time while supplying points in the velocity-period plane separated by not more than twenty seconds in period. The modes calculated for each iteration were; ${}_0S_{25}$ to ${}_0S_{40}$, every third mode, ${}_0S_{40}$ to ${}_0S_{96}$, every tenth mode, ${}_0S_{40}$ to ${}_0S_{526}$, every thirtieth mode, ${}_0T_{25}$ to ${}_0T_{46}$, every third mode, ${}_0T_{45}$ to ${}_0T_{105}$, every tenth mode, and ${}_0T_{105}$ to ${}_0T_{495}$, every thirtieth mode. Linear interpolation between these points gives the velocity values at the periods corresponding to data points. The final models were calculated for more densely packed modes so interpolation to the data would be more accurate.

Changes in the models are chosen to reduce the deviation between data and model. At each iteration at least one and usually not more that three parameters were changed. Occasionally several parameters were changed simultaneously by the same relative amount. This has the effect of varying one parameter and requiring that its ratio with each of the other changed parameters remain constant.

Each of the data sets was fitted by making minimal changes from the appropriate P.R.E.M. type starting model. An attempt was made to keep the variations of parameters with age smooth but as an iterative forward modeling technique was used no formal smoothness criteria was applied. To keep the number of parameters small, an experiment where parameters were successively freed was conducted and is described in the following paragraphs. The

effect of each of the possible parameters on the dispersion curves was calculated and the tradeoffs between parameters noted. This will be discussed later. Considering the number of parameters, the correlations between them, and the limited resolution of the data, the non-uniqueness resulting from the underdetermined nature of the problem will make physical interpretations of the resulting models somewhat speculative. However, this type of procedure can be useful in testing the validity of any theoretical upper mantle model that can be suitably formulated.

To determine a proper parameterization a series of experiments with different parameters was performed. The average ocean data of Mitchell and Yu [1980] were modeled by successively freeing each parameter. LID thickness and isotropic LID velocity were varied to produce a set of parametric curves in the two parameters. A six kilometer anisotropic layer was placed at the top of the lid to make the model consistent with observed P_n velocities and to improve the fit at short periods. To reduce model velocities to values near the data the mean SH velocity in the LVZ was decreased while VSH/VSV, VSH/VPH, and VPH/VPV were held constant. This magnified the changes due to lid thickness and velocity. The magnification is caused by the increased contrast in velocity across the LID LVZ discontinuity. To resolve inconsistencies which prevented simultaneous fitting of Love and Rayleigh wave data, particularly at periods below 100 seconds, the velocities in the LID and the LVZ were decoupled such that only VSV/VPV and VSH/VPH ratios remained constant, that is VSV/VSH was allowed to vary. Then the gradients of velocity and ETA were varied in the LVZ and the means and gradients of velocity were completely decoupled. To improve the fits at shorter periods the crustal velocity, crustal thickness, water thickness, and sediment thickness were varied. These variations were small ,a couple of percent maximum, but they dramatically improved the fit for periods less than about 80

seconds. Thus the parameters investigated are these:

(1): water depth

(2): sediment thickness

(3): crustal velocity; the crust is assumed to be isotropic and the velocities in the two layers are varied by the same relative amount.

(4-5): crustal thickness; the two crustal layers are separately varied

(6): lid thickness; 6 km upper layer , thickness of remaining lid to be determined

(7-8): lid velocity; VSV/VPV and VSH/VPH are held constant, VSH and VSV are allowed to vary in the lower lid layer, velocities in the upper lid layer are fixed to be consistent with P_n data.

(9-13): mean VSH, VSV, VPH, VPV, and ETA in the LVZ

(14-18): gradient of VSH, VSV, VPH, VPV in the LVZ

(19): Mean VSH between 220 and 400 km. VSH/VPH, VSV/VPV, and VSH/VPV are held constant.

Each of the nineteen parameters discussed above produce specific changes to the phase and group velocity dispersion curves. There exist several tradeoffs between these parameters that make the models non-unique within the error of the data. However, some tradeoffs can be limited by the application of constraints. The partial derivatives of the dispersion curves with respect to each of the above parameters were determined by differencing the Love and Rayleigh phase and group velocities calculated in two almost identical models. The two models differed in only one parameter. The resulting estimates of the partial derivatives are shown in figures 9 to 12. The correlations between them and their behavior are discussed in detail below.

Variations in parameters associated with the water layer, the sediment layer, and the crustal layers are interrelated. Varying the depth of the water

and sediment layers causes the curvature of the dispersion curves to change at periods less then 45 seconds. For an increase in the water or sediment thickness the reduction in phase velocity increases as period decreases since short periods are more sensitive to the near surface velocity perturbations. Crustal thickness was increased by about 6.5%, and crustal velocity was increased by 5%. Increasing the crustal thickness at the expense of the faster LVZ means a net decrease in velocity in the depth range between the bottom of the old crust and the top of the new LVZ. Thus, the sharp decrease in group and phase velocities at periods less than 45 seconds is reasonable as is the sharp increase in the same period range when the velocity of the crust is increased. The partial derivatives in figures 9 to 12 show that comparable effects at short period result when crustal velocity increases and when crustal thickness decreases, although, the former has a larger effect at periods of 50-100 seconds. Also a similar effect occurs at short period(<45 seconds) when water depth is decreased. Observed values of water depth and crustal thickness and velocity are used to bound the models derived in this study.

The effects of variations in the parameters associated with the lid are changes in the dispersion curves that are most obvious at periods less than 100 seconds but are easily measurable at all periods considered. Increasing VSV and VPV in the LID causes a small but sharp increase in Love wave phase and group velocity at periods <60 seconds and a steep increase in Rayleigh velocities for periods <100 seconds. Decreasing VSH and VPH in the LID causes a small decrease in Rayleigh velocities and a larger decrease in Love velocities. It is important to note that changes in LID velocity must be weighted by the LID thickness to determine the correct perturbations to improve the fit of the model. The partial derivatives shown are for a increase in the mean velocities of 3% for SV and PV and for a decrease in the mean velocities of 3% for SH and PH.

The effects of variation of the five parameters associated with the mean velocities and mean ETA in the LVZ are strongly interrelated. The mean of each velocity in the LVZ was increased about 5% and the mean of ETA was increased about 2%. This translates to an increase of 0.4 km/s in P velocity, 0.2 km/s in S velocity, and 0.02 in ETA. The resulting partial derivatives show that Rayleigh waves are most sensitive to VSV, as expected, but they also show that Rayleigh waves are sensitive to VPV and VPH and ETA at a significant level, while the effect of VSH is an order of magnitude smaller. In contrast the Love waves are most sensitive to VSH, as expected, but are also sensitive to VSV. This illustrates one of the problems of the pseudo- isotropic procedure. In an anisotropic earth Rayleigh waves have a significant dependence on P velocities and on VSH velocity and Love waves have a significant dependence on SV velocity. The problem is coupled rather than separable as required by the pseudo-isotropic procedure.

The effects of variations in the five gradient parameters associated with the LVZ are strongly interrelated and are intimately related to the effects for changes in the mean parameters. The effects of changing the gradients in the LVZ while keeping the means constant was to produce partial derivatives of the same sign as changing the corresponding mean for periods greater than about 100 seconds, and to produce partial derivatives of the opposite sign for periods less than 100 seconds. The relative magnitudes of the contributions of each of the velocity gradients was in proportion to the contributions from the corresponding means. Tradeoffs exist between groups of velocities and velocity gradients in the LVZ but they involve complex combinations of several parameters. To illustrate the possible tradeoffs a discussion of two equally well fitting models to the average oceanic data is presented below. Decreasing the thickness of the LID will increase the thickness of the LVZ and will proportionately increase the effects of the parameters in the LVZ. This means that the

thickness of the LID has more effect than the direct partial derivative in thickness indicates.

The procedure used to forward model each data set considered magnitudes, shapes, and interrelations of the partial derivatives of the parameters. In order to find a model to fit each data set within a specified uncertainty while adjusting the smallest number of parameters the following procedure was used:

(1): Assign values for water, sediment and crustal parameters appropriate for a given data set (eg. water and sediment thicknesses from Leeds Knopoff and Kausel (1974), or crustal structures from Yu and Mitchell (1979), and Forsyth (1975a))

(2): If necessary adjust mean SH velocity in the LVZ or between 220 and 400 km, keeping VSH/VPH, VSH/VSV, and VSV/VPV ratios constant, to fit the longer periods. To keep the variation of velocities with age as smooth as possible the magnitudes of changes in the two regions can be traded off.

(3): Adjust the thickness, the velocities, and ETA of the lid to fit the data as well as possible.

(4): If necessary adjust the gradients of velocity and ETA in the LVZ keeping all ratios constant.

(5): If necessary decouple the means and gradients of the velocities and ETA in the LVZ such that VSH/VPH and VSV/VPV remain constant and VSH/VSV is allowed to vary.

(6): If necessary decouple VSH/VPH and VSV/VPV

(7): If necessary fine tune by returning to 3 and repeating the process until the fit is at the desired level of accuracy.

(8): Fine tune the fit at short periods by varying water, sediment, and crustal velocity. The changes should be small if any are needed.

The problem of non-uniqueness is particularly obvious when using this type of method. Very different models can fit the data to within comparable standard deviations. As an example of this, two models that fit the average ocean data with comparable standard deviations are discussed below. The two velocity depth profiles are shown in figure 13. Except for the SH velocities the models are quite different. There are substantial differences in the means of the other three velocities in the LVZ and the corresponding three velocity gradients differ in sign. The gradients of ETA are also different. While the fits of these two models to the data, shown in figures 3 and 4, are not identical the standard deviations of the two sets of residuals are comparable. The Rayleigh residuals are given in table 3 and 4 and shown if figure 14. The Love residuals are given in tables 5 and 6 and shown in figure 15.

The standard deviation of the residuals are given in table 18; S is the standard deviation giving each point equal weight, SW is a weighted standard deviation where the weights are proportional to the distances in period between adjacent points. The latter statistic should remove any bias caused by unequal distribution of data points in period, and is determined from the following relations:

$$SW^2 = \frac{\sum_{i=1}^{n} f_i T_i - \left[\sum_{i=1}^{n} f_i\right] \overline{T}^2}{\sum_{i=1}^{n} f_i - 1}$$

where $\overline{T} = \dfrac{\sum_{i=1}^{n} T_i}{n}$

$$f_1 = \left|T_2 - T_1\right|$$

$$f_n = \left|T_n - T_{n-1}\right|$$

$$f_{i+1} = \frac{\left|T_{i+1} - T_{i-1}\right|}{2} \quad \text{for } i = 1, \ldots, n-1$$

For Rayleigh phase velocities model B fits better at shorter periods and model A fits better at longer periods. Overall, model B is a slightly better fit but the difference of about 1.4% should not be significant. For Rayleigh wave group velocities model A gives a significantly better fit. For Love wave phase velocities model B gives a marginally better fit and for Love wave group velocities the quality of fit is essentially identical. A small change in the SH velocities of model A would increase the Love residuals so that the two model would give equal standard deviations, and such a change increases the difference between the two models. Thus, quite different models can fit the data to the same accuracy.

DISCUSSION

The models derived using the method described above are shown in figures 16 through 20. Calculated Rayleigh and Love wave phase and group velocities are listed in tables 1 through 14. In this section the models resulting from each of the data sets and some possible implications arising from them will be discussed. The most striking difference from previous studies, common to all models, is the thickness of the lithosphere. The lithosphere , defined here as the LID plus the crust, is much thinner than the lithosphere derived in isotropic seismic studies and is comparable in thickness to the flexural lithosphere defined by Watts et. al. [1980]. Also, the variation of anisotropy with age in the regionalized oceanic data sets indicate that this method can be used to test models of mantle flow based on the hypothesis of aligned olivine crystals. The

regionalized oceanic data sets of Mitchell and Yu [1980] and Forsyth [1975a] both show an increase in lithosphere thickness with age, and variations in lithosphere and LVZ velocities and ETA values with age.

The average Earth velocity model is presented in figure 16 and in table 17, the phase and group velocities at the periods of the data are given in tables 1 and 2. The average Earth model is similar to P.R.E.M. Above 18.4 km and below 220 km no changes have been made. The major difference is the introduction of a constant velocity LID region between 18.4 and 46.8 km depth. This causes a large increase in velocity between the bottom of the P.R.E.M crust at 24 km and the bottom of the average Earth model crust at 18.4 km. Thus, the mean velocities and ETA values over the depth range of the LID are increased by about 2-4% for velocities and decreased about 2.7% for ETA. The introduction of the LID reduces the depth extent of the LVZ. Mean velocities in the LVZ increased by 0.1-1.5% for SH, PH, and PV and decreased by 0.25% for SV. The range of the velocities and ETA values in the LVZ increase by about 12% for SH and PH to 0.018 km/s and 0.015 km/s respectively and decreased considerably for SV and PV. to about 0.012 km/s. These changes provide a better fit than P.R.E.M. to the short period fundamental mode data.

Figures 1 and 2 show that this model fits the fundamental mode data well. Overall the residuals have a mean of -0.0031 ± 0.0102 km/s. The residuals, given in tables 1 and 2, show that data from different sources have systematic differences. The model consistently lies below the data of Fukao and Kobayashi [1983] except for shorter period Love phase velocities. It is within the quoted uncertainty of the data 96% of the time. The data of Nakanishi and Anderson [1983] were added after the model was derived. They show residuals that are generally smaller than the other data sets. However, the extremely small standard deviations of the data cause more than half the points to be separated

from the model by more than 2σ. The model lies consistently above the Rayleigh phase velocity data of Mills and Hales [1977]. Their Rayleigh wave data set lies within their quoted uncertainties 83% of the time.

The average ocean model is shown in figure 13 and given in table 15. The model shown in dotted lines, model B, is most similar to P.R.E.M. The dispersion curves resulting from this model are shown in figure 4, and the phase and group velocities at the periods of the data points are given in tables 3 to 6. There are several major differences between P.R.E.M. and the model for average ocean. First, the water layer is thicker since it is not being averaged over the entire surface of the Earth. Also, the crustal layers are thinner since the thicker continental crust is not being included in the average. Therefore, there is a net decrease in velocity of 13.6% for S and 9.1% for P caused by the additional thickness of the slow water layer and to a lesser extent to the decreased thickness of the faster crustal layers. Finally, a LID was introduced, between 12 km and 53 km. Since, between 12 km and 24.4 km the average ocean LID corresponds to the slower crustal layers in P.R.E.M. the oceanic model's LID is faster by 11.4% for PV, 10.1% for PH, 12.0% for SV, 9.3% for SH, and 5.0% for ETA when compared to the mean velocities over the same depth ranges in P.R.E.M. In the LVZ the means of velocity and ETA increase slightly. For PV, PH, and SH slopes became steeper, and for SV and ETA slopes were reduced.

Figure 4 shows how this model fits the fundamental mode data set. Again the different data sets show systematic differences. The data of Mitchell and Yu [1980] are well fit with the Love wave velocities and the Rayleigh wave phase velocities lying consistently above the data and the Rayleigh wave group velocities lying consistently below the data. The data of Kanamori are well fit by the model. All points lie within 1.1 σ. The Rayleigh wave group velocity data of Dziewonski and Steim [1983] all are fit by the model at a 2σ level, and 55% lie

within 1σ. The model lies consistently above the Rayleigh wave phase velocity data of Mills and Hales [1978a] and fits at the 2σ level. Overall, the residuals have a mean of 0.0024 ± 0.0212 km/s, with 81% of points falling within 1σ. Thus, this is a good fit to the data.

The models for the regions used by Mitchell and Yu [1980] and Forsyth [1975a] show an increase in the thickness of the lithosphere with age. Particularly for the younger provinces of Mitchell and Yu [1980] the models fit much better than those previously proposed. The models were derived by trying to make a smooth variation with age in as many parameters as possible. The average ocean model included in this series of models is model A which fits smoothly into the progression of parameters in the regional models. This average ocean model was derived using only the data of Mitchell and Yu [1980]. It is reasonable to assume that a set of models similar to the alternate average ocean model could be derived to fit as well as, or better than, the models presented here.

The velocity depth models for the 0-20 M.Y. and 20-50 M.Y. old oceanic regions are shown in figure 17 and given in table 15, the phase and group velocities and the residuals are given in tables 7 and 8, and the corresponding dispersion curves are shown in figure 5. The data of Mitchell and Yu [1980] are well fit. For the younger region Love group velocities tend to fall below the model at short periods and above it at longer (>70s) periods. The model lies consistently 1-2 σ below the Rayleigh wave phase velocity data of Wielandt and Knopoff for periods >180s. Below that period the data is fit at a 1σ level and there is no systematic bias. For the older region the model fits both data sets well.

The velocity depth models for 50-100 M.Y. and >100 M.Y. old oceanic regions are given in figure 18 and table 15, corresponding velocities are given in tables 9 and 10, and dispersion curves are shown in figure 6. For both data sets the phase velocities are very well fit and the model tends to lie above the data for

longer period Love phase velocities and below it for shorter periods. Group velocities do not fit as well but still agree well with the data at a 2σ level. The data of Souriau and Souriau [1983] added after the model was derived, fit at a 2σ level and add data coverage between 102 and 300 seconds for the >100 M.Y. old region. The uncertainties of group velocity points at a given period are smaller for the older regions. The poorer fits mentioned above are judged with respect to those uncertainties. Thus, although the absolute residuals are comparable the agreement between data points and the model appears to be poorer for older regions where uncertainties are smaller.

The velocity depth models for 0-5 M.Y. and 5-10 M.Y. old oceanic regions are given in figure 19 and table 16, the corresponding dispersion curves are shown in figure 7, and the velocities and residuals are given in tables 11 and 12. The velocity depth models for 10-20 M.Y. and 0-10 M.Y old oceanic regions are given in figure 20 and table 16, the corresponding dispersion curves are given in figure 8, and the velocities and residuals are given in tables 13 and 14. These four models fit the data quite well. There appear to be no systematic trends in the relationship of data and models.

The differences between the regionalized models can be interpreted as a progression of some physical properties with age. First, the thickness of the LID increases with age from 16 km for 0-5 M.Y. old oceanic regions of the Nazca plate to 26 km for the corresponding 10-20 M.Y. old regions, and from 20 km in the 0-20 M.Y. old oceanic regions of the Pacific to 50 km in the Pacific oceanic region >100 M.Y. in age. A somewhat thicker LID might be accommodated by adjusting the other parameters but inserting a LID of the thickness found in most other studies would be difficult, if possible at all, using this approach. The differences in lithospheric thickness between typical previously accepted models and the models presented here are small for young regions and increasingly serious as

the ocean floor increases in age. The variation of LID thicknuss with age is shown in figure 21. This figure also shows the estimates by Watts et. al. [1980] of the thickness of the elastic or flexural lithosphere. Next, the lid velocity increases with age for all but the two oldest provinces. In these two oldest regions the lid velocity becomes anisotropic with vertical velocities slower than horizontal velocities. Also, the water and sediment layers increase in depth with age, the crustal thickness is allowed to increase slightly after 20 M.Y., and the crustal velocities decrease slightly after 50 M.Y. Up to 20 M.Y. age the crustal thicknesses and velocities are unchanged. Thereafter, changes are small and result from fine tuning the fits at very short periods (<50s). The dispersion data, for old ocean, could alternately be fit by further increasing crustal and sediment thickness, or water depth. However, by using reasonable observational estimates as constraints on these thicknesses the velocity decrease in the crust seems necessary. The gradients of SH and PV velocity increase with age. Many of the trends such as increasing lid velocity, increasing SH and PH velocities at the top of the lid, etc. are not continued into the >100 M.Y old province of Mitchell and Yu [1980]. A possible reason for this is the presence of many oceanic plateau areas in the old ocean region. Inclusion of such slow structures would reduce the average velocities for the region causing the progression of velocities with age to be broken. The lateral heterogeneity introduced by plateau regions might also account for the need to introduce anisotropy in the lid of the homogeneous but anisotropic model.

The thickness of the lithosphere is an important parameter in the theory of plate tectonics. The seismic lithosphere, sometimes called the LID, has previously been calculated to be at least 100 km thick for oceanic regions >100 M.Y. in age. This value is commonly accepted and is often adopted as the thickness of the slab, or plate. The plate is considered to translate coherently in most

plate tectonic models. Thermal cooling models of the aging plate have also sometimes been based on this thickness. In turn these thermal models are used to determine thermal properties of the LID or, if thermal properties are assumed, to determine the thickness of a thermal lithosphere. The thickness of the plate is also important when modeling convection and other physical processes in a subduction zone. However, in subduction zones there are some independent evidences for thinner lithosphere. For example a thin LID was inferred from long range refraction measurements in the western Pacific [Nagumo et. al., 1981; see triangle in figure 21]. It is also interesting to note that the separation of the earthquakes in the double Wadati-Benioff zone in Japan [Hasegawa et. al., 1978], if interpreted as the thickness of the subducting LID, is comparable to the LID thickness derived in this study. It has also been observed that the lithosphere in the region of some hot spots is thinner than predicted by the age of the lithosphere in question. This has been interpreted as a thermal resetting of thickness due to the hot spot [Detrick and Crough, 1978]. However, these measurements could also be used to support the hypothesis that the seismic lithosphere is thinner than previously believed, as derived by anisotropic modelling. If further studies of other types of data can verify the thicknesses found for the models presented here, and by Anderson and Regan [1983], then many accepted interpretations and ideas will need to be reconsidered.

The thickness of the elastic lithosphere has been determined by studying phenomena such as seamount loading [Watts et. al., 1980]. Generally it is believed that the elastic lithosphere rapidly thickens with age to a thickness of about 30 km for seafloor 50 M.Y. in age. Thereafter, the thickness seems to increase more slowly. Previous estimates of the thickness of the seismic lithosphere, based on isotropic calculations, agreed that it was considerably thicker

than the elastic lithosphere. The difference was reconciled by discussing the different phenomena involved in determining the thicknesses. Each phenomena was discussed in terms of relaxation times [Anderson and Minster, 1980] for relaxation by dislocation glide and climb. For this type of interpretation the thickness of the lithosphere is defined as the depth having a characteristic time equal to the duration of the load. Relaxation times generally decrease with depth as temperature increases. For high stress, long duration loads, such as seamount loading and post glacial rebound, the thickness of the lithosphere is small and the relaxation time is long. For low stress short duration seismic waves relaxation times in and and for some distance below the thin flexural lithosphere are long compared to seismic periods. Thus, the seismic lithosphere is thicker than the elastic lithosphere in a homogeneous mantle. The relaxation time is strongly dependent on the temperature and stress. Thus, the thickness of the flexural or seismic lithosphere is highly dependent on the temperature and stress profiles.

The interpretation discussed above is based on dislocation glide and climb which are both thermally activated processes. Thus, the relation between flexural and elastic lithosphere thicknesses is dependent on temperature. However, the strength and other rheological properties of the lithosphere also depend on mineralogy, crystal structure and orientation, stress, partial melting, and duration of load. If temperature is not the dominant parameter, as could be the case if the upper mantle is chemically layered with the base of the LID corresponding to a change in crystal structure or mineralogy, the elastic and seismic lithospheres might be of the same thickness.

The variation of velocities and anisotropy with age suggests that interpreting the results in terms of stress or flow aligned olivine [Nicolas and Poirier, 1976] is a promising approach [Regan and Anderson, 1981]. Using such an

approach the velocities depend primarily on temperature, pressure and crystal orientation. The effects of each of these variables will be discussed below. The basis of an interpretation based on flow and the resulting velocity depth relations are illustrated in figure 22. The upper left diagram schematically illustrates a convection cell with material rising at the midocean ridge (R) and flowing down at the trench (T).

In the lower left of figure 22 is the schematic temperature profile for such a cell. The seismic velocities decrease with temperature and increase with pressure as depth increases. Combining the effects of temperature and pressure one obtains a relation between velocity and depth. At the ridge the temperature increases very rapidly with depth near the surface. Thus, the effects of temperature dominate over those of pressure and velocities decrease. Deeper levels under the ridge are almost isothermal. Thus, the effect of pressure dominates and the velocities increase. At the trench the temperature gradient is large near the base of the cell and nearly isothermal at shallower depths. Therefore, the velocity response is a mirror image of that at the ridge. Midway between the ridge and the trench (M) the temperature increases rapidly near the top and bottom of the cell. Thus, the velocities decrease rapidly in these regions.

The crystal orientation, if alignment with flow is assumed, is with the shortest and slowest axis (b-axis) perpendicular to the flow. Thus, at the ridge and the trench where the flow is vertical the b-axis is horizontal, and midway between where the flow is horizontal the b-axis is vertical. The following discussion considers the effects of crystal orientation alone in a flowing olivine aggregate. VPH and VSH midway between the upward and downward flowing edges of the convection cell are controlled by the velocities along the a-axis and c-axis; VPV and VSV depend on the velocity along the b-axis . Thus, at the midpoint, and wherever flow is horizontal, SH>SV and PH>PV. At the ridge and at the

trench the flow is vertical, rapidly changing to horizontal at the top and bottom of the cell. For vertical flow the horizontal velocity is controlled by the b-axis and c-axis velocities so SH<SV and PH<PV. The values at the top and bottom of the cell rapidly change to the horizontal flow values. Between the midpoint and the trench or ridge the transition from horizontal to vertical flow velocities becomes sharper and the depth extent of constant vertical velocities increases.

Combining the effects of temperature and pressure with the effect of orientation requires a calculation of the magnitude of each of the effects. The values of the elastic parameters and their derivatives with pressure and temperature have been measured for olivine and fosterite [Graham and Barsch, 1969; Kumazawa and Anderson, 1969], and for olivine rich rocks [Christensen and Crossen, 1968; Christensen and Smewing, 1981]. To determine the size of the velocity gradients caused by pressure and temperature effects these measured values were substituted into the following relation that defines the temperature derivative of velocity.

$$\frac{dV}{dT} = \frac{\partial V}{\partial P}\frac{\partial P}{\partial z} + \frac{\partial V}{\partial T}\frac{\partial T}{\partial z}$$

The temperature profile shown in fig 22 was used to determine $\frac{\partial T}{\partial z}$. The measured values of the elastic constants give the magnitude of the orientation effect. Thus, the two effects can be combined to produce velocity profiles like those shown in figure 22.

Comparing this model to the derived velocity depth structures for the regionalized oceanic provinces shows that it could be a viable interpretation. For the average ocean model and for the upper 100 km of the mantle in the youngest regions PH>PV and SH>SV. This is consistent with horizontal flow. For the 100-220 km depth range for the youngest regions (0-5, 5-10) SH>SV The

vertical flow expected in the ridge crest environment would exhibit this behavior. The temperature gradients implied by the measured values of $\frac{\partial V}{\partial P}$ and $\frac{\partial V}{\partial T}$, and the values of $\frac{dV}{dT}$ from the models are 5-8 degrees Centigrade per kilometer for older ocean and are consistent with reorientation of olivine along with a small temperature gradient for younger oceanic regions. Note that with these temperature and flow models the velocity of Love waves along ridges is extremely slow and the velocity of Rayleigh waves is high along subduction zones. For midplate locations Love wave velocities are higher and Rayleigh wave velocities are lower than at plate boundaries. The results of this study indicate that a model derived on the basis of flow aligned olivine could be fitted by existing data with small changes to the present models.

Acknowledgments. We thank Adam Dziewonski for use of a program, and Jeff Given for his assistance. This research was supported by National Science Foundation grant number EAR811-5236 and National Aeronautics and Space Administration grant number NSG-7610. Contribution number 4015, Division of Geological and Planetary Sciences, California Institute of Technology, Pasadena, California 91125.

REFERENCES

Anderson, Don L., Recent evidence concerning the structure and composition of the Earth's mantle, *Physics and Chemistry of the Earth, 6.*,Pergamon Press, Oxford, 1-131, 1966.

Anderson, Don L., Dziewonski, A. M., Upper mantle anisotropy: Evidence from free oscillations, *Geophys. J. R. Astron. Soc., 69*, 383-404, 1982.

Anderson, Don L., Hart, R., An Earth Model Based on Free Oscillations and Body Waves, *J. Geophys. Res., 81*, 1461-1475, 1976.

Anderson, Don L., Minster, B., Seismic Velocity, Attenuation and Rheology of the Mantle: in Source Mechanism and Earthquake Prediction, C. J. Allegre (Ed), Centre National de la recherche scientifique, Paris, 13-22, 1980.

Anderson, Don L., Regan J., Uppermantle Anisotropy and the Oceanic Lithosphere, *Geophys. Res. Lett., 10*, 841-844, 1983.

Christensen, N. I., Crossen, R. S., Seismic Anisotropy in the Upper Mantle, *Tectonophysics, 6*, 93-107, 1968.

Christensen, N. I., Smewing, J. O., Geology and Seismic Structure of the Northern Section of the Oman Ophiolite, *J. Geophys. Res., 86*, 2545-2555, 1981.

Crampin, S., A Comment on "The Early Structural Evolution and Anisotropy of the Oceanic Upper Mantle", *Geophys. J. R. Astron. Soc., 46*, 193-197, 1976.

Crampin, S., King, D. W., Evidence for anisotropy in the upper mantle beneath Eurasia from the polarization of higher mode seismic surface waves, *Geophys. J. R. Astron. Soc., 49*, 59-85, 1977.

Detrick, R. S., Crough, S. T., Island Subsidence, Hot Spots, and Lithosphere Thinning, *J. Geophys. Res.*, *83*, 1236-1244, 1978.

Dziewonski, A. M., On Regional Differences in the Dispersion of Mantle Rayleigh Waves, *Geophys. J. R. Astron. Soc.*, *22*, 289-325, 1970.

Dziewonski, A. M., Anderson, Don L., Preliminary reference Earth model, *Phys. Earth Planet. Inter.*, *25*, 297-356, 1981.

Dziewonski, A. M., Gilbert, F., Observations of Normal Modes from 84 Recordings of the Alaskan Earthquake of 1964 March 28, *Geophys. J. R. Astron. Soc.*, *27*, 393-446, 1972.

Dziewonski, A. M., Steim, S., Dispersion and attenuation of mantle waves through waveform inversion, *Geophys. J. R. Astron. Soc.*, *70*, 503-527, 1982.

Forsyth, D. W., The Early Structural Evolution and Anisotropy of the Oceanic Upper Mantle, *Geophys. J. R. Astron. Soc.*, *43*, 103-162, 1975a.

Forsyth, D. W., A New Method for The Analysis of Multi-Mode Surface Wave Dispersion: Application to Love Wave Propagation in the Pacific, *Bull. Seism. Soc. Amer.*, *65*, 323-342, 1975b.

Fukao, Y., Kobayashi, M., Phase and group velocities and Q of mantle Love and Rayleigh waves of the first two modes and their azimuthal dependences for the 1963 Kurile Islands Earthquake, (in press).

Graham, E. K., Barsch, G. R., Elastic Constants of Single-Crystal Forsterite as a Function of Temperature and Pressure, *J. Geophys. Res.*, *74*, 5949-5960, 1969.

Hasegawa, A., Umino, N., Takagi, A., Double-Planed Structure of the Deep Seismic Zone in the Northeastern Japan Arc, *Tectonophysics*, *47*, 43-58, 1978.

Jordan, T., Anderson, Don. L., Earth Structure From Free Oscillations and Travel Times, *Geophys. J. R. Astron. Soc.*, *36*, 411-459, 1974.

Kanamori, H., Velocity and Q of the Mantle Waves, *Phys. Earth Planet. Inter.*, *2*, 259-275, 1970.

Kirkwood, S., The significance of isotropic inversion of anisotropic surface-wave dispersion, *Geophys. J. R. Astron. Soc.*, *55*, 131-142, 1978.

Kumazawa, M., Anderson O. L., Elastic Moduli, Pressure Derivatives and Temperature Derivatives of Single-Crystal Olivine and Single-Crystal Forsterite, *J. Geophys. Res.*, *74*, 5961-5972, 1969.

Leeds, A. R., Knopoff, L., Kausel, E. G., Variations in Upper Mantle Structure under the Pacific Ocean, *Science*, *186*, 141-143, 1974.

Leveque, J. J., Regional upper mantle S velocity models from phase velocities of great-circle Rayleigh waves, *Geophys. J. R. Astron. Soc.*, *63*, 23-43, 1980.

Love, A. E. H., *A Treatise on the Mathematical Theory of Elasticity*, 4th edn. Cambridge University Press, Cambridge, 643 pp.

Mills, J. M., Hales, A. L., Great-Circle Rayleigh Wave Attenuation and Group Velocity, Part I: Observations for Periods Between 150 and 600 Seconds for Seven Great-Circle Paths, *Phys. Earth. Planet. Int.*, *14*, 109-119, 1977.

Mills, J. M., Hales, A. L., Great-Circle Rayleigh Wave Attenuation and Group Velocity, Part II: Observations for Periods Between 50 and 200 Seconds for Nine Great-Circle Paths and Global Averages for Periods of 50 to 600 Seconds, *Phys. Earth. Planet. Int.*, *17*, 209-231, 1978a.

Mills, J. M., Hales, A. L., Great-Circle Rayleigh Wave Attenuation and Group Velocity, Part IV: Regionalization of Pure Path Models for Shear Velocity and Attenuation, *Phys. Earth. Planet. Int.*, *17*, 323-352, 1978b.

Mitchell, B. J., Yu, G., Surface wave dispersion, regionalized velocity models, and anisotropy of the Pacific crust and upper mantle, *Geophys. J. R. Astron. Soc.*, *63*, 497-514, 1980.

Montagner, J. P., Jobert, N., Variation with age of the deep structure of the Pacific Ocean inferred from very long period Rayleigh wave dispersion, *Geophys. Res.Let.*, *10*, 273-276, 1983.

Nagumo, S., Ouchi, T., Kasahara, J., Koresawa, S., Tomada, Y., Kobayashi, K., Furumoto, A. S., Odegard, M. E., Sutton, G. H., Sub-Moho seismic profile of the Maricena Basin; ocean bottom seismograph long range explosion experiment, *Earth Planet. Sci. Lett.*, *53*, 93-102, 1981.

Nakanishi, I., Phase velocity and Q of mantle Rayleigh waves, *Geophys. J. R. Astron. Soc.*, *58*, 35-59, 1979.

Nakanishi, I, Shear velocity and shear attenuation model inverted from world wide and pure path average data of mantle Rayleigh waves (${}_0S_{25}$ to ${}_0S_{80}$) and fundamental spheroidal modes (${}_0S_2$ to ${}_0S_{24}$), *Geophys. J. R. Astron. Soc.*, *66*, 83-130, 1981.

Nakanishi, I., Anderson, D. L., World Wide Distribution of Group Velocity of Mantle Rayleigh Waves as Determined by Spherical Harmonic Inversion, *Bull. Seismol. Soc. Amer.*, *72*, 1185-1194, 1982.

Nakanishi, I., Anderson, D. L., Aspherical Heterogeneity of the Mantle from Phase Velocities of Mantle Waves, (in press).

Nakanishi, I., Anderson, D. L., Measurements of Mantle wave velocities and inversion for lateral heterogeneity and anisotropy Part I: Analysis of Great-circle phase velocities, (in press).

Nakanishi, I., Anderson, D. L., Measurements of Mantle wave velocities and inversion for later heterogeneity and anisotropy Part II: Analysis by the single station method, (in press).

Nicolas, A., Poirier, J. P., Crystalline Plasticity and Solid State Flow in Metamorphic Rocks, *Wiley Inter-Science*, London, 437pp.

Okal, E. A., The effect of intrinsic oceanic upper-mantle heterogeneity on regionalization of long-period Rayleigh wave phase velocities, *Geophys. J. R. Astron. Soc.*, *49*, 357-370, 1977.

Regan, J., Anderson, D. L., Mapping Mantle Flow with Seismic Anisotropy, *EOS*, *62*, 1024, 1981.

Schlue, J. W., Knopoff, L., Shear-wave polarization anisotropy in the Pacific Basin, *Geophys. J. R. Astron. Soc.*, *49*, 145-165, 1977.

Schlue, J. W., Knopoff, L., Inversion of surface-wave phase velocities for an anisotropic structure, *Geophys. J. R. Astron. Soc.*, *54*, 697-702, 1978.

Silver, P. G., Jordan, T. H., Fundamental spheroidal mode observations of aspherical heterogeneity, *Geophys. J. R. Astron. Soc.*, *64*, 605-634, 1981.

Souriau, A., Souriau, M., Test of tectonic models by great-circle Rayleigh waves, *Geophys. J. R. Astron. Soc.*, *73*, 533-551, 1983.

Takeuchi, H., Saito, M., Seismic Surface Waves, in *Seismology: Surface Waves and Earth Oscillations*, pp. 217-295, ed. Bolt, B. A., *Methods in Computational Physics*, *11*, New York, Academic Press, 1972.

Toksoz, N., Anderson, D. L., Phase Velocities of Long Period Surface Waves and Structure of the Upper Mantle, *J. Geophys. Res.*, *71*, 1649-1658, 1966.

Watts, A., Bodine, J. H., Steckler, M. S., Observations of Flexure and the State of Stress in the Oceanic Lithosphere, *J. Geophys. Res.*, *85*, 6369-6376, 1980.

Wielandt, R., Knopoff, L., Dispersion of Very Long Period Rayleigh Waves Along the East Pacific Rise: Evidence for S-Wave Velocity Anomalies to

450 km Depth, *J. Geophys. Res.*, *87*, 8631-8641, 1982.

Wu, F. T., Mantle Rayleigh Wave Dispersion and Tectonic Provinces, *J. Geophys. Res.*, *77*, 6445-6453, 1972.

Yu, G., Mitchell, B. J., Regionalized shear velocity models of the Pacific upper mantle from observed Love and Rayleigh wave dispersion, *Geophys. J. R. Astron. Soc.*, *57*, 311-341, 1979.

TABLE 1
RAYLEIGH WAVE VELOCITIES FOR THE AVERAGE EARTH MODEL

N	T	C_o	C	±	$C-C_o$	N	T	U_o	U	±	$U-U_o$
	(s)	km/s	km/s	km/s	km/s		(s)	km/s	km/s	km/s	km/s
4	400.00	5.9445	5.9269	0.0033	-0.0176	1	399.61	4.3789	4.3571	0.0496	-0.0218
1	399.61	5.9396	5.9247	0.0178	-0.0149	2	389.54	4.3100	4.2891	0 0017	-0.0209
2	389.54	5.8721	5.8675	0.0012	-0.0046	1	372.36	4.1794	4.1728	0.0530	-0.0066
1	372.36	5.7794	5.7692	0.0126	-0.0102	2	360.04	4.1090	4.0886	0.0017	-0.0204
2	360.04	5.7016	5.6950	0.0012	-0.0066	1	348.60	4.0090	4.0110	0.0458	0.0020
1	348.60	5.6354	5.6227	0.0118	-0.0127	2	335.72	3.9440	3.9261	0.0016	-0.0179
2	335.72	5.5459	5.5378	0.0011	-0.0081	1	324.44	3.8696	3.8557	0.0360	-0.0139
4	333.33	5.5257	5.5214	0.0013	-0.0042	2	315.20	3.8160	3.8018	0.0015	-0.0142
1	324.44	5.4740	5.4605	0.0107	-0.0135	1	300.62	3.7360	3.7265	0.0280	-0.0095
2	315.20	5.4042	5.3953	0.0011	-0.0089	3	300.00	3.7301	3.7235	0.0190	-0.0066
1	300.62	5.3030	5.2896	0.0113	-0.0134	4	298.76	3.7316	3.7175	0.0106	-0.0141
3	300.00	5.2830	5.2850	0.0041	0.0020	2	297.54	3.7220	3.7120	0.0015	-0.0100
2	297.54	5.2760	5.2670	0.0200	-0.0090	3	290.00	3.6665	3.6837	0.0190	0.0172
3	290.00	5.2113	5.2109	0.0049	-0.0004	3	280.00	3.6540	3.6461	0.0230	-0.0079
4	285.71	5.1853	5.1789	0.0007	-0.0064	1	275.36	3.6440	3.6287	0.0200	-0.0153
1	275.36	5.1130	5.1019	0.0104	-0.0111	2	274.99	3.6330	3.6278	0.0200	-0.0052
2	274.99	5.1077	5.0991	0.0200	-0.0086	4	274.63	3.6334	3.6270	0.0014	-0.0064
2	255.95	4.9650	4.9576	0.0100	-0.0074	3	270.00	3.6142	3.6169	0.0110	0.0027
1	254.02	4.9540	4.9436	0.0110	-0.0104	3	260.00	3.5937	3.5950	0.0060	0.0013
4	250.00	4.9187	4.9145	0.0060	-0.0042	2	255.95	3.5860	3.5865	0.0100	0.0005
3	250.00	4.9131	4.9145	0.0064	0.0014	1	254.02	3.5940	3.5847	0.0180	-0.0093
3	239.92	4.8362	4.8414	0.0063	0.0052	4	252.46	3.5849	3.5833	0.0060	-0.0016
2	239.50	4.8447	4.8385	0.0100	-0.0062	3	250.00	3.5772	3.5810	0.0070	0.0038
1	227.56	4.7650	4.7552	0.0099	-0.0098	3	240.00	3.5667	3.5719	0.0050	0.0052
3	225.49	4.7340	4.7408	0.0062	0.0068	2	239.50	3.5710	3.5716	0.0100	0.0006
2	225.08	4.7426	4.7380	0.0100	-0.0046	4	232.08	3.5716	3.5718	0.0010	0.0002
4	222.22	4.7217	4.7189	0.0005	-0.0028	3	230.00	3.5736	3.5719	0.0050	-0.0017
3	212.62	4.6487	4.6549	0.0100	0.0062	1	227.56	3.5770	3.5719	0.0170	-0.0051
2	212.27	4.6563	4.6526	0.0100	-0.0037	2	225.08	3.5700	3.5721	0.0100	0.0021
3	201.16	4.5746	4.5820	0.0100	0.0074	3	220.00	3.5805	3.5755	0.0080	-0.0050
1	201.03	4.5880	4.5812	0.0097	-0.0068	2	212.27	3.5780	3.5808	0.0100	0.0028
2	200.81	4.5826	4.5798	0.0100	-0.0028	3	210.00	3.5836	3.5833	0.0080	-0.0003
4	200.00	4.5764	4.5749	0.0005	-0.0015	1	201.03	3.5970	3.5932	0.0210	-0.0038
3	190.83	4.5112	4.5194	0.0100	0.0082	2	200.81	3.5910	3.5935	0.0100	0.0025
2	190.48	4.5184	4.5173	0.0014	-0.0011	3	200.00	3.5943	3.5946	0.0100	0.0003
4	181.82	4.4679	4.4694	0.0005	0.0015	4	196.11	3.5990	3.5999	0.0009	0.0009
2	181.15	4.4568	4.4657	0.0013	0.0089	3	190.00	3.5908	3.6084	0.0090	0.0176
2	172.66	4.4161	4.4188	0.0013	0.0027	2	181.15	3.6230	3.6226	0.0100	-0.0004
1	168.91	4.4010	4.3981	0.0119	-0.0029	4	180.28	3.6226	3.6240	0.0009	0.0014
4	166.67	4.3846	4.3857	0.0006	0.0011	3	180.00	3.5987	3.6245	0.0130	0.0258
3	162.74	4.3536	4.3640	0.0200	0.0104	2	172.66	3.6350	3.6362	0.0100	0.0012
5	157.75	4.3377	4.3395	0.0010	0.0018	3	170.00	3.6176	3.6405	0.0120	0.0229
4	153.85	4.3201	4.3205	0.0006	0.0004	1	168.91	3.6450	3.6422	0.0280	-0.0028
3	151.50	4.2963	4.3091	0.0084	0.0128	4	165.72	3.6485	3.6474	0.0010	-0.0011
4	142.86	4.2678	4.2671	0.0013	-0.0007	3	160.00	3.6464	3.6567	0.0170	0.0103
3	141.64	4.2499	4.2612	0.0091	0.0113	4	152.34	3.6743	3.6694	0.0011	-0.0049
1	140.64	4.2660	4.2566	0.0157	-0.0094	3	150.00	3.6761	3.6733	0.0160	-0.0028
4	133.33	4.2250	4.2247	0.0006	-0.0003	1	140.64	3.7140	3.6889	0.0470	-0.0251
3	131.33	4.2042	4.2159	0.0098	0.0117	4	140.04	3.6987	3.6899	0.0012	-0.0088
3	125.24	4.1781	4.1893	0.0103	0.0112	3	140.00	3.7004	3.6900	0.0170	-0.0104
4	125.00	4.1900	4.1882	0.0009	-0.0018	3	130.00	3.7079	3.7064	0.0170	-0.0015

TABLE 1(cont)
RAYLEIGH WAVE VELOCITIES FOR THE AVERAGE EARTH MODEL

N	T	C_o	C	±	$C-C_o$	N	T	U_o	U	±	$U-U_o$
	(s)	km/s	km/s	km/s	km/s		(s)	km/s	km/s	km/s	km/s
4	117.65	4.1610	4.1588	0.0007	-0.0022	4	128.73	3.7236	3.7085	0.0014	-0.0151
3	112.19	4.1249	4.1369	0.0121	0.0120	3	120.00	3.7399	3.7229	0.0140	-0.0170
4	111.11	4.1370	4.1328	0.0008	-0.0042	4	118.34	3.7480	3.7256	0.0016	-0.0224
4	105.26	4.1155	4.1112	0.0009	-0.0043	3	110.00	3.7588	3.7295	0.0023	-0.0193
3	101.57	4.0841	4.0976	0.0147	0.0135	4	108.78	3.7695	3.7416	0.0018	-0.279
1	101.45	4.1110	4.0971	0.0150	-0.0139	1	101.45	3.8010	3.7541	0.0480	-0.0469
4	100.00	4.0973	4.0921	0.0010	-0.0052	4	100.00	3.7881	3.7566	0.0022	-0.0315
3	92.75	4.0521	4.0672	0.0195	0.0151	3	100.00	3.7720	3.7566	0.0045	-0.0154
3	73.48	3.9910	4.0086	0.0400	0.0176	3	90.00	3.7974	3.7742	0.0085	-0.0232
3	60.78	3.9556	3.9759	0.0300	0.0203	3	80.00	3.7998	3.7921	0.0031	-0.0077
3	50.00	3.9600	3.9510	0.0310	-0.0090	3	70.00	3.8024	3.8089	0.0044	0.0065
						3	60.00	3.8360	3.8232	0.0031	-0.0148
						3	50.00	3.8850	3.8286	0.0031	-0.0564

References:
N=1 Fukao and Kobayashi (1983)
N=2 Dziewonski and Steim (1982)
N=3 Mills and Hales (1977; 1978a)
N=4 Nakanishi and Anderson (1983)

TABLE 2
LOVE WAVE VELOCITIES FOR THE AVERAGE EARTH MODEL

N	T	C_o	C	±	$C-C_o$	N	T	U_o	U	±	$U-U_o$
	(s)	km/s	km/s	km/s	km/s		(s)	km/s	km/s	km/s	km/s
2	400.00	5.5498	5.5435	0.0032	-0.0063	1	399.61	4.5238	4.5113	0.0432	-0.0125
1	399.61	5.5443	5.5422	0.0192	-0.0021	1	372.36	4.4850	4.4737	0.0431	-0.0113
1	372.36	5.4607	5.4562	0.0177	-0.0045	1	348.60	4.4539	4.4456	0.0416	-0.0083
1	348.61	5.3860	5.3805	0.0176	-0.0055	2	325.00	4.4173	4 4229	0.0041	0.0056
2	333.33	5.3360	5.3316	0.0021	-0.0044	1	324.44	4.4301	4.4225	0.0345	-0.0076
1	324.44	5.3110	5.3031	0.0170	-0.0079	1	300.62	4.4123	4.4049	0.0282	-0.0074
3	310.63	5.2599	5.2589	0.0026	-0.0010	2	298.76	4.4048	4.4038	0.0030	-0.0010
1	300.62	5.2336	5.2269	0.0173	-0.0066	1	275.36	4.4000	4.3922	0.0260	-0.0078
3	290.77	5.1950	5.1956	0.0025	0.0006	2	274.63	4.3968	4.3918	0.0023	-0.0050
2	285.71	5.1826	5.1797	0.0014	-0.0029	1	254.02	4.3931	4.3855	0.0266	-0.0076
1	275.36	5.1520	5.1469	0.0170	-0.0051	2	252.46	4.3917	4.3850	0.0019	-0.0067
3	273.27	5.1398	5.1403	0.0025	0.0005	2	232.08	4.3887	4.3818	0.0017	-0.0069
3	265.30	5.1150	5.1154	0.0025	0.0004	1	227.56	4.3860	4.3815	0.0282	-0.0045
1	254.02	5.0840	5.0802	0.0160	-0.0038	2	213.34	4.3874	4.3811	0.0016	-0.0063
3	250.66	5.0700	5.0697	0.0025	-0.0003	1	201.03	4.3853	4.3815	0.0288	-0.0038
2	250.00	5.0713	5.0677	0.0012	-0.0036	2	196.11	4.3865	4.3819	0.0015	-0.0046
3	231.56	5.0110	5.0111	0.0025	0.0001	2	180.28	4.3852	4.3834	0.0015	-0.0018
1	227.56	5.0010	4.9990	0.0170	-0.0020	1	169.78	4.3931	4.3848	0.0278	-0.0083
2	222.22	4.9867	4.9829	0.0012	-0.0038	2	165.72	4.3855	4.3854	0.0015	-0.0001
3	215.17	4.9610	4.9617	0.0025	0.0007	2	152.34	4.3853	4.3872	0.0015	0.0019
1	201.03	4.9200	4.9199	0.0180	-0.0001	1	140.64	4.3976	4 3886	0.0259	-0.0090
3	200.95	4.9190	4.9197	0.0024	0.0007	2	140.04	4.3854	4.3887	0.0016	0.0033
2	200.00	4.9195	4.9169	0.0011	-0.0026	2	128.73	4.3851	4.3900	0.0017	0.0049
3	188.51	4.8820	4.8835	0.0024	0.0015	2	118.34	4.3849	4.3907	0.0018	0.0058
2	181.82	4.8656	4.8644	0.0010	-0.0012	2	108.78	4.3866	4.3909	0.0019	0.0043
3	181.04	4.8600	4.8622	0.0024	0.0022	1	101.45	4.4060	4.3908	0.0260	-0.0152
1	169.78	4.8290	4.8309	0.0190	0.0019	2	100.00	4.3870	4.3907	0.0022	0.0037
2	166.67	4.8214	4.8222	0.0011	0.0008						
3	158.95	4.7970	4.8007	0.0024	0.0037						
2	153.85	4.7851	4.7865	0.0011	0.0014						
3	151.04	4.7750	4.7787	0.0024	0.0037						
2	142.86	4.7545	4.7568	0.0011	0.0023						
1	140.64	4.7510	4.7509	0.0220	-0.0001						
1	133.33	4.7285	4.7314	0.0011	0.0029						
3	129.51	4.7190	4.7212	0.0029	0.0022						
2	125.00	4.7061	4.7094	0.0012	0.0033						
2	117.63	4.6867	4.6903	0.0012	0.0036						
2	111.11	4.6693	4.6734	0.0013	0.0041						
2	105.00	4.6542	4.6578	0.0013	0.0036						
1	101.45	4.6460	4.6487	0.0210	0.0027						
2	100.00	4.6405	4.6450	0.0014	0.0045						

References:
N=1 Fukao and Kobayashi (1983)
N=2 Nakanishi and Anderson (1983)
N=3 Dziewonski and Anderson (1981)

TABLE 3
RAYLEIGH WAVE PHASE VELOCITY FOR TWO AVERAGE OCEAN MODELS

N	T	C_0	C_B	C_A	±	$C_B - C_0$	$C_A - C_0$
	(s)	km/s	km/s	km/s	km/s	km/s	km/s
1	300.00	5.3010	5.3079	5.2988	0.0140	0.0069	-0.0022
3	297.25	5.2811	5.2873	5.2781	0.0260	0.0062	-0.0030
1	275.00	5.1320	5.1204	5.1108	0.0110	-0.0116	-0.0212
3	274.73	5.1125	5.1184	5.1088	0.0031	0.0059	-0.0037
3	255.72	4.9695	4.9756	4.9654	0.0030	0.0061	-0.0041
1	250.00	4.9290	4.9335	4.9231	0.0160	0.0045	-0.0059
3	239.30	4.8487	4.8549	4.8439	0.0029	0.0062	-0.0048
1	225.00	4.7450	4.7534	4.7416	0.0100	0.0084	-0.0034
3	224.90	4.7464	4.7527	4.7410	0.0033	0.0063	-0.0054
3	212.12	4.6596	4.6657	4.6531	0.0033	0.0061	-0.0065
3	200.67	4.5858	4.5912	4.5777	0.0037	0.0054	-0.0081
1	200.00	4.5880	4.5870	4.5735	0.0130	-0.0010	-0.0145
3	190.34	4.5228	4.5268	4.5127	0.0041	0.0040	-0.0101
3	180.99	4.4681	4.4734	4.4584	0.0044	0.0053	-0.0097
1	175.00	4.4420	4.4391	4.4236	0.0110	-0.0029	-0.0184
3	172.54	4.4194	4.4251	4.4093	0.0048	0.0057	-0.0101
3	164.83	4.3758	4.3811	4.3645	0.0057	0.0053	-0.0113
1	150.00	4.3250	4.3045	4.2871	0.0320	-0.0205	-0.0379
2	102.40	4.0820	4.0994	4.0815	0.0180	0.0174	-0.0005
2	93.10	4.0510	4.0690	4.0521	0.0190	0.0180	0.0011
2	81.90	4.0250	4.0406	4.0258	0.0190	0.0156	0.0008
2	70.60	4.0050	4.0150	4.0026	0.0190	0.0100	-0.0024
2	60.00	3.9940	3.9996	3.9900	0.0190	0.0056	-0.0040
2	51.20	3.9910	3.9940	3.9870	0.0190	0.0030	-0.0040
2	40.00	3.9960	3.9967	3.9927	0.0200	0.0007	-0.0033
2	35.30	4.0010	4.0010	3.9978	0.0200	0.0000	-0.0032
2	60.00	3.9940	3.9996	3.9900	0.0190	0.0056	-0.0040
2	51.20	3.9910	3.9940	3.9870	0.0190	0.0030	-0.0040
2	40.00	3.9960	3.9967	3.9927	0.0200	0.0007	-0.0033
2	35.30	4.0010	4.0010	3.9978	0.0200	0.0000	-0.0032
2	30.00	4.0060	4.0073	4.0044	0.0200	0.0013	-0.0016
2	28.00	4.0070	4.0094	4.0063	0.0200	0.0024	-0.0007
2	26.00	4.0060	4.0106	4.0073	0.0200	0.0046	0.0013
2	24.00	4.0040	4.0099	4.0063	0.0200	0.0059	0.0023
2	22.00	3.9970	4.0051	4.0014	0.0200	0.0081	0.0044

References:
N=1 Kanamori (1970)
N=2 Mitchell and Yu (1980)
N=3 Mills and Hales (1978b)

TABLE 4
RAYLEIGH WAVE GROUP VELOCITIES FOR TWO AVERAGE OCEAN MODELS

N	T (s)	C_o km/s	C_B km/s	C_A km/s	± km/s	$C_B - C_o$ km/s	$C_A - C_o$ km/s
2	300.00	3.6457	3.7360	3.7263	0.0745	0.0903	0.0806
3	297.25	3.7260	3.7252	3.7152	0.0057	-0.0008	-0.0108
2	280.00	3.6394	3.6574	3.6455	0.0117	0.0180	0.0061
3	274.73	3.6350	3.6367	3.6244	0.0057	0.0017	-0.0106
2	260.00	3.6213	3.6013	3.5872	0.0813	-0.0200	-0.0341
3	255.72	3.5880	3.5911	3.5766	0.0057	0.0031	-0.0114
2	240.00	3.5979	3.5732	3.5563	0.0532	-0.0247	-0.0416
3	239.30	3.5690	3.5724	3.5556	0.0058	0.0034	-0.0134
3	224.90	3.5680	3.5692	3.5503	0.0064	0.0012	-0.0177
2	220.00	3.5611	3.5712	3.5516	0.0352	0.0101	-0.0095
3	212.12	3.5790	3.5746	3.5538	0.0071	-0.0044	-0.0252
3	200.67	3.5950	3.5842	3.5619	0.0086	-0.0108	-0.0331
2	200.00	3.6010	3.5849	3.5626	0.0369	-0.0161	-0.0384
3	190.34	3.6150	3.5957	3.5723	0.0112	-0.0193	-0.0427
2	190.00	3.5906	3.5961	3.5728	0.0416	0.0055	-0.0178
3	180.99	3.6310	3.6088	3.5849	0.0110	-0.0222	-0.0461
2	180.00	3.6365	3.6102	3.5863	0.0232	-0.0263	-0.0502
3	172.54	3.6410	3.6207	3.5963	0.0131	-0.0203	-0.0447
2	170.00	3.6439	3.6243	3.5998	0.0319	-0.0196	-0.0441
3	164.83	3.6520	3.6316	3.6067	0.0168	-0.0204	-0.0453
2	160.00	3.6366	3.6390	3.6144	0.0306	0.0024	-0.0222
2	150.00	3.6457	3.6558	3.6320	0.0354	0.0101	-0.0137
2	140.00	3.6823	3.6730	3.6503	0.0464	-0.0093	-0.0320
2	130.00	3.7201	3.6930	3.6725	0.0376	-0.0271	-0.0476
2	120.00	3.7329	3.7150	3.6976	0.0303	-0.0179	-0.0353
2	110.00	3.7588	3.7400	3.7265	0.0341	-0.0188	-0.0323
1	110.00	3.7600	3.7400	3.7265	0.0320	-0.0200	-0.0335
2	100.00	3.7105	3.7694	3.7603	0.0470	0.0589	0.0498
1	100.00	3.7740	3.7694	3.7603	0.0270	-0.0046	-0.0137
1	90.00	3.8120	3.8040	3.8000	0.0220	-0.0080	-0.0120
2	90.00	3.7841	3.8040	3.8000	0.0553	0.0199	0.0159
1	80.00	3.8580	3.8433	3.8442	0.0230	-0.0147	-0.0138
2	80.00	3.7848	3.8433	3.8442	0.0763	0.0585	0.0594
1	70.00	3.9000	3.8837	3.8896	0.0190	-0.0163	-0.0104
2	70.00	3.8975	3.8837	3.8896	0.0781	-0.0138	-0.0079
1	60.00	3.9460	3.9270	3.9373	0.0190	-0.0190	-0.0087
2	60.00	3.9860	3.9270	3.9373	0.0920	-0.0590	-0.0487
1	50.00	3.9980	3.9703	3.9831	0.0230	-0.0277	-0.0149
2	50.00	3.9256	3.9703	3.9831	0.1134	0.0447	0.0575
1	45.00	4.0200	3.9914	4.0046	0.0230	-0.0286	-0.0154
1	40.00	4.0390	4.0112	4.0238	0.0150	-0.0278	-0.0152
1	36.00	4.0300	4.0245	4.0362	0.0230	-0.0055	0.0062
1	32.00	4.0340	4.0322	4.0432	0.0240	-0.0018	0.0092
1	28.00	4.0060	4.0240	4.0362	0.0260	0.0180	0.0302
1	24.00	3.9340	3.9761	3.9959	0.0310	0.0421	0.0619
1	20.00	3.8030	3.8004	3.8507	0.0470	-0.0026	0.0477
1	18.00	3.7290	3.7159	3.7827	0.0910	-0.0131	0.0537

References:
N=1 Mitchell and Yu (1980)
N=2 Mills and Hales (1978b)
N=3 Dziewonski and Steim (1982)

TABLE 5
LOVE WAVE PHASE VELOCITIES FOR TWO AVERAGE OCEAN MODELS

N	T	C_0	C_B	C_A	±	$C_B - C_0$	$C_A - C_0$
	(s)	km/s	km/s	km/s	km/s	km/s	km/s
1	300.0	5.236	5.230	5.218	0.018	-0.006	-0.018
1	275.0	5.157	5.152	5.139	0.016	-0.005	-0.018
1	250.0	5.074	5.074	5.061	0.014	0.000	-0.013
1	225.0	4.993	4.999	4.985	0.016	0.006	-0.008
1	200.0	4.929	4.926	4.912	0.017	-0.003	-0.017
1	175.0	4.858	4.858	4.841	0.016	-0.002	-0.017
1	150.0	4.791	4.788	4.774	0.015	-0.003	-0.018
1	125.0	4.753	4.725	4.710	0.021	-0.028	-0.043
2	102.4	4.669	4.671	4.655	0.024	0.002	-0.014
2	93.1	4.643	4.650	4.634	0.024	0.007	-0.009
2	81.9	4.616	4.625	4.609	0.023	0.009	-0.007
2	70.6	4.590	4.602	4.585	0.023	0.012	-0.005
2	60.0	4.570	4.581	4.564	0.021	0.011	-0.006
2	51.2	4.547	4.564	4.547	0.022	0.017	0.000
2	40.0	4.527	4.545	4.528	0.023	0.018	0.001
2	35.3	4.509	4.538	4.521	0.023	0.029	0.012
2	30.0	4.492	4.530	4.513	0.024	0.038	0.021

References:
N=1 Kanamori (1970)
N=2 Mitchell and Yu (1980)

TABLE 6
LOVE WAVE GROUP VELOCITIES FOR TWO AVERAGE OCEAN MODELS

N	T	C_g	C_B	C_A	±	$C_B - C_g$	$C_A - C_g$
	(s)	km/s	km/s	km/s	km/s	km/s	km/s
2	110.0	4.416	4.429	4.411	0.032	0.013	-0.005
2	100.0	4.412	4.433	4.415	0.038	0.021	0.003
2	90.0	4.426	4.438	4.420	0.035	0.012	-0.006
2	80.0	4.438	4.443	4.425	0.030	0.005	-0.013
2	70.0	4.468	4.449	4.431	0.031	-0.019	-0.037
2	60.0	4.464	4.455	4.437	0.034	-0.009	-0.027
2	50.0	4.449	4.461	4.444	0.037	0.012	-0.006
2	45.0	4.434	4.465	4.447	0.033	0.031	0.013
2	40.0	4.437	4.468	4.450	0.030	0.031	0.013
2	36.0	4.432	4.471	4.452	0.029	0.039	0.021
2	32.0	4.412	4.47	4.455	0.035	0.061	0.043

Reference: N=2 Mitchell and Yu (1980)

TABLE 7
VELOCITIES FOR 0-20 M.Y. OLD OCEANIC REGION

RAYLEIGH

N	T	C_o	C	±	$C-C_o$	N	T	U_o	U	±	$U-U_o$
	(s)	km/s	km/s	km/s	km/s		(s)	km/s	km/s	km/s	km/s
1	300.0	5.239	5.253	0.012	0.014	2	110.0	3.602	3.645	0.040	0.043
1	273.0	5.033	5.049	0.011	0.016	2	100.0	3.669	3.666	0.035	-0.003
1	248.0	4.841	4.861	0.010	0.020	2	90.0	3.683	3.691	0.028	0 008
1	225.0	4.676	4.695	0.010	0.019	2	80.0	3.683	3.719	0.029	0.036
1	204.0	4.537	4.552	0.009	0.015	2	70.0	3.714	3.747	0.023	0.033
1	186.0	4.428	4.441	0.009	0.013	2	60.0	3.767	3.777	0.024	0.010
1	169.0	4.335	4.342	0.008	0.007	2	50.0	3.809	3.805	0.028	-0.004
1	153.0	4.254	4.255	0.008	0.001	2	45.0	3.841	3.820	0.028	-0.021
1	139.0	4.186	4.185	0.008	-0.002	2	40.0	3.862	3.836	0.027	-0.026
1	126.0	4.123	4.123	0.007	0.000	2	36.0	3.884	3.852	0.028	-0.032
1	115.0	4.078	4.076	0.007	-0.002	2	32.0	3.901	3.872	0.030	-0.029
1	104.0	4.034	4.032	0.007	-0.002	2	28.0	3.899	3.895	0.033	-0.005
2	102.4	4.031	4.025	0.024	-0.006	2	24.0	3.889	3.918	0.040	0.029
1	95.0	3.999	3.999	0.007	-0.001	2	20.0	3.840	3.931	0.062	0.091
2	93.1	3.999	3.992	0.024	-0.007	2	18.0	3.766	3.931	0.118	0.165
1	86.0	3.970	3.970	0.007	0.000	2	16.0	3.512	3.930	0.145	0.418
2	81.9	3.966	3.958	0.025	-0.008						
1	78.0	3.944	3.946	0.007	0.002						
1	71.0	3.927	3.927	0.007	-0.000						
2	70.6	3.914	3.926	0.024	0.012						
1	65.0	3.914	3.913	0.007	-0.001						
2	60.0	3.890	3.902	0.025	0.012						
1	59.0	3.900	3.901	0.007	0.001						
1	53.0	3.890	3.890	0.007	0.000						
2	51.2	3.875	3.888	0.025	0.013						
1	48.0	3.883	3.884	0.009	0.001						
1	44.0	3.883	3.879	0.011	-0.004						
1	40.0	3.886	3.876	0.013	-0.010						
2	40.0	3.866	3.876	0.025	0.010						
2	35.3	3.868	3.874	0.025	0.006						
2	30.0	3.875	3.875	0.026	-0.000						
2	28.0	3.877	3.876	0.027	-0.001						
2	26.0	3.877	3.878	0.026	0.001						
2	24.0	3.882	3.881	0.025	-0.001						
2	22.0	3.881	3.884	0.025	0.003						
2	20.0	3.879	3.888	0.026	0.009						

LOVE

N	T	C_o	C	±	$C-C_o$	N	T	U_o	U	±	$U-U_o$
	(s)	km/s	km/s	km/s	km/s		(s)	km/s	km/s	km/s	km/s
2	300.0	5.156	5.149	0.031	-0.007	2	110.0	4.352	4.335	0.043	-0.017
2	275.0	5.056	5.069	0.031	0.013	2	100.0	4.376	4.339	0.051	-0.073
2	250.0	5.000	4.990	0.031	-0.011	2	90.0	4.384	4.345	0.048	-0.039
2	225.0	4.920	4.912	0.031	-0.008	2	80.0	4.374	4.350	0.041	-0.042
2	200.0	4.845	4.838	0.031	-0.007	2	70.0	4.413	4.357	0.040	-0.056
2	175.0	4.784	4.767	0.031	-0.017	2	60.0	4.331	4.364	0.043	0.033
2	150.0	4.705	4.698	0.031	-0.007	2	50.0	4.363	4.372	0.049	0.009
2	125.0	4.641	4.633	0.031	-0.008	2	45.0	4.351	4.376	0.044	0.025
2	102.4	4.559	4.578	0.031	0.019	2	40.0	4.290	4.380	0.039	0.090

TABLE 7(cont)
VELOCITIES FOR 0-20 M.Y. OLD OCEANIC REGION
LOVE

N	T	C_o	C	±	$C-C_o$	N	T	U_o	U	±	$U-U_o$
	(s)	km/s	km/s	km/s	km/s		(s)	km/s	km/s	km/s	km/s
2	93.1	4.534	4.557	0.031	0.023	2	36.00	4.298	4.384	0.037	0.086
2	81.9	4.515	4.532	0.031	0.017	2	32.00	4.381	4.388	0.047	0.007
2	70.6	4.498	4.508	0.030	0.010						
2	60.0	4.477	4.487	0.028	0.010						
2	51.2	4.470	4.471	0.030	0.001						
2	40.0	4.447	4.452	0.031	0.005						
2	35.3	4.426	4.445	0.031	0.019						
2	30.0	4.390	4.438	0.032	0.048						

References:
N=1 Wielandt and Knopoff (1982)
N=2 Mitchell and Yu (1980)

TABLE 8
VELOCITIES FOR 20-50 M.Y. OLD OCEANIC REGION

RAYLEIGH

N	T	C_o	C	±	$C-C_o$	N	T	U_o	U	±	$U-U_o$
	(s)	km/s	km/s	km/s	km/s		(s)	km/s	km/s	km/s	km/s
1	142.9	4.254	4.233	0.052	-0.021	1	137.0	3.539	3.651	0.062	0.112
1	123.0	4.131	4.145	0.026	0.014	1	122.0	3.684	3.681	0.045	-0.003
1	111.1	4.089	4.097	0.017	0.008	2	110.0	3.724	3.708	0.032	-0.016
2	102.4	4.065	4.065	0.018	0.000	1	101.5	3.693	3.729	0.028	0.036
1	100.0	4.053	4.057	0.014	0.004	2	100.0	3.714	3.733	0.027	0.019
2	93.1	4.027	4.034	0.019	0.007	1	94.3	3.755	3.750	0.029	-0.005
1	90.9	4.025	4.029	0.013	0.004	2	90.0	3.758	3.763	0.022	0.005
2	81.9	3.999	4.004	0.019	0.005	2	83.3	3.776	3.786	0.019	0.010
1	77.0	3.998	3.991	0.010	-0.007	2	80.0	3.785	3.797	0.023	0.012
2	70.6	3.975	3.977	0.019	0.002	1	73.5	3.808	3.819	0.016	0.011
1	66.7	3.970	3.970	0.009	0.000	2	70.0	3.828	3.832	0.019	0.004
2	60.0	3.959	3.959	0.019	-0.000	1	64.9	3.840	3.852	0.013	0.012
1	58.8	3.960	3.958	0.008	-0.002	2	60.0	3.875	3.871	0.019	-0.004
2	51.2	3.950	3.950	0.019	0.000	1	57.5	3.884	3.882	0.012	-0.002
1	50.0	3.952	3.950	0.008	-0.002	1	50.8	3.939	3.910	0.014	-0.029
2	40.0	3.953	3.950	0.020	-0.003	2	50.0	3.935	3.914	0.023	-0.021
1	40.0	3.959	3.950	0.008	-0.009	2	45.0	3.969	3.936	0.023	-0.033
2	35.3	3.958	3.954	0.020	-0.004	1	44.6	3.963	3.938	0.016	-0.025
1	33.3	3.966	3.957	0.009	-0.010	2	40.0	4.001	3.959	0.002	-0.042
2	30.0	3.966	3.962	0.021	-0.004	1	39.4	3.986	3.962	0.018	-0.024
2	28.0	3.969	3.965	0.021	-0.004	2	36.0	4.018	3.978	0.023	-0.040
2	26.0	3.971	3.969	0.021	-0.002	1	34.8	4.001	3.984	0.019	-0.018
1	25.0	3.979	3.971	0.011	-0.009	2	32.0	4.022	3.995	0.024	-0.027
2	24.0	3.971	3.971	0.020	0.001	1	30.8	3.993	3.999	0.020	0.006
2	22.0	3.971	3.973	0.020	0.002	2	28.0	4.004	4.005	0.026	0.001
2	20.0	3.965	3.970	0.021	0.005	1	27.1	3.977	4.005	0.020	0.028
1	20.0	3.959	3.970	0.012	0.011	2	24.0	3.943	3.991	0.031	0.048
						1	23.9	3.943	3.991	0.021	0.048
						1	21.5	3.893	3.953	0.025	0.060
						2	20.0	3.839	3.901	0.047	0.062

LOVE

N	T	C_o	C	±	$C-C_o$	N	T	U_o	U	±	$U-U_o$
	(s)	km/s	km/s	km/s	km/s		(s)	km/s	km/s	km/s	km/s
2	102.4	4.595	4.586	0.024	-0.009	2	110.0	4.336	4.341	0.032	0.005
2	93.1	4.570	4.565	0.024	-0.006	2	100.0	4.341	4.345	0.038	0.004
2	81.9	4.537	4.540	0.023	0.003	2	90.0	4.332	4.350	0.035	0.018
2	70.6	4.511	4.516	0.023	0.005	2	80.0	4.386	4.356	0.030	-0.031
2	60.0	4.497	4.495	0.021	-0.002	2	70.0	4.435	4.361	0.031	-0.074
2	51.2	4.476	4.478	0.022	0.002	2	60.0	4.466	4.367	0.034	-0.099
2	40.0	4.456	4.458	0.023	0.002	2	50.0	4.403	4.373	0.037	-0.030
2	35.3	4.434	4.451	0.023	0.017	2	45.0	4.358	4.376	0.033	0.018
2	30.0	4.413	4.442	0.024	0.029	2	40.0	4.375	4.378	0.030	0.003
						2	36.0	4.407	4.380	0.029	-0.027
						2	32.0	4.411	4.381	0.035	-0.030

References:
N=1 Forsyth(1975a)
N=2 Mitchell and Yu (1980)

TABLE 9
VELOCITIES FOR 50-100 M.Y. OLD OCEANIC REGION

RAYLEIGH

N	T	C_o	C	±	$C-C_o$	N	T	U_o	U	±	$U-U_o$
	(s)	km/s	km/s	km/s	km/s		(s)	km/s	km/s	km/s	km/s
1	102.4	4.098	4.097	0.012	-0.001	1	110.0	3.796	3.766	0.022	-0.030
1	93.1	4.075	4.071	0.013	-0.004	1	100.0	3.834	3.808	0.019	-0.026
1	81.9	4.051	4.051	0.013	-0.001	1	90.0	3.866	3.856	0.016	-0.010
1	70.6	4.037	4.033	0.013	-0.004	1	80.0	3.931	3.907	0.016	-0.024
1	60.0	4.028	4.027	0.013	-0.001	1	70.0	3.973	3.958	0.013	-0.015
1	51.2	4.032	4.029	0.013	-0.003	1	60.0	4.016	4.009	0.014	-0.007
1	40.0	4.039	4.039	0.014	0.000	1	50.0	4.061	4.051	0.016	-0.010
1	35.3	4.044	4.044	0.014	0.000	1	45.0	4.071	4.067	0.016	-0.004
1	30.0	4.045	4.047	0.014	0.002	1	40.0	4.077	4.077	0.015	-0.000
1	28.0	4.045	4.046	0.014	0.001	1	36.0	4.042	4.077	0.015	0.035
1	26.0	4.041	4.043	0.014	0.002	1	32.0	4.047	4.065	0.016	0.018
1	24.0	4.036	4.035	0.014	-0.001	1	28.0	4.007	4.028	0.017	0.021
1	22.0	4.022	4.020	0.014	-0.002	1	24.0	3.924	3.931	0.020	0.007
1	20.0	3.988	3.990	0.014	0.002	1	20.0	3.767	3.639	0.030	-0.128

LOVE

N	T	C_o	C	±	$C-C_o$	N	T	U_o	U	±	$U-U_o$
	(s)	km/s	km/s	km/s	km/s		(s)	km/s	km/s	km/s	km/s
1	175.0	4.908	4.901	0.021	-0.007	1	110.0	4.496	4.491	0.028	-0.005
1	150.0	4.841	4.836	0.021	-0.005	1	100.0	4.484	4.496	0.033	0.012
1	125.0	4.803	4.775	0.021	-0.029	1	90.0	4.519	4.502	0.031	-0.017
1	102.4	4.743	4.723	0.021	-0.020	1	80.0	4.489	4.507	0.026	0.018
1	93.1	4.716	4.703	0.021	-0.013	1	70.0	4.502	4.514	0.026	0.012
1	81.9	4.694	4.680	0.020	-0.014	1	60.0	4.462	4.520	0.028	0.058
1	70.6	4.669	4.658	0.020	-0.011	1	50.0	4.495	4.526	0.031	0.031
1	60.0	4.643	4.638	0.018	-0.005	1	45.0	4.51	4.529	0.029	0.019
1	51.2	4.618	4.623	0.019	0.005	1	40.0	4.499	4.532	0.026	0.033
1	40.0	4.597	4.605	0.020	0.008	1	36.0	4.456	4.535	0.024	0.079
1	35.3	4.584	4.598	0.020	0.014	1	32.0	4.414	4.536	0.029	0.122
1	30.0	4.570	4.591	0.021	0.021						

Reference: N=1 Mitchell and Yu (1980)

TABLE 10
VELOCITIES FOR >100 M.Y. OLD OCEANIC REGION

RAYLEIGH

N	T	C_o	C	±	$C-C_o$	N	T	U_o	U	±	$U-U_o$
	(s)	km/s	km/s	km/s	km/s		(s)	km/s	km/s	km/s	km/s
2	300.0	5.288	5.316	0.008	0.028	1	110.0	3.854	3.843	0.023	-0.011
2	275.0	5.114	5.130	0.008	0.016	1	100.0	3.883	3.877	0.019	-0.006
2	250.0	4.926	4.945	0.006	0.019	1	90.0	3.916	3.912	0.016	-0.004
2	225.0	4.760	4.768	0.007	0.009	1	80.0	3.953	3.950	0.016	-0.003
2	200.0	4.593	4.606	0.007	0.013	1	70.0	4.008	3.986	0.013	-0.022
2	175.0	4.454	4.465	0.007	0.011	1	60.0	4.056	4.019	0.014	-0.038
2	160.0	4.374	4.385	0.010	0.011	1	50.0	4.071	4.040	0.016	-0.031
2	150.0	4.350	4.339	0.015	-0.012	1	45.0	4.069	4.041	0.015	-0.028
2	125.0	4.260	4.232	0.040	-0.028	1	40.0	4.049	4.035	0.015	-0.015
1	102.4	4.146	4.157	0.012	0.011	1	36.0	4.018	4.019	0.015	0.001
1	93.1	4.122	4.133	0.013	0.011	1	32.0	3.972	3.987	0.015	0.015
1	81.9	4.097	4.111	0.013	0.014	1	28.0	3.901	3.922	0.016	0.021
1	70.6	4.085	4.091	0.013	0.006	1	24.0	3.781	3.773	0.018	-0.008
1	60.0	4.081	4.081	0.013	-0.000	1	20.0	3.546	3.316	0.026	-0.230
1	51.2	4.076	4.077	0.013	0.001						
1	40.0	4.072	4.073	0.014	0.001						
1	35.3	4.065	4.070	0.014	0.005						
1	30.0	4.052	4.058	0.014	0.006						
1	28.0	4.042	4.050	0.014	0.008						
1	26.0	4.032	4.038	0.014	0.006						
1	24.0	4.017	4.019	0.013	0.002						
1	22.0	3.986	3.989	0.013	0.003						
1	20.0	3.954	3.935	0.013	-0.019						

LOVE

N	T	C_o	C	±	$C-C_o$	N	T	U_o	U	±	$U-U_o$
	(s)	km/s	km/s	km/s	km/s		(s)	km/s	km/s	km/s	km/s
1	102.4	4.686	4.684	0.017	-0.002	1	110.0	4.512	4.446	0.025	-0.066
1	93.1	4.665	4.663	0.018	-0.002	1	100.0	4.531	4.451	0.029	-0.081
1	81.9	4.646	4.639	0.017	-0.007	1	90.0	4.517	4.456	0.027	-0.061
1	70.6	4.622	4.616	0.017	-0.006	1	80.0	4.478	4.461	0.022	-0.017
1	60.0	4.602	4.595	0.016	-0.007	1	70.0	4.490	4.467	0.023	-0.023
1	51.2	4.586	4.579	0.017	-0.007	1	60.0	4.504	4.473	0.025	-0.032
1	40.0	4.560	4.560	0.017	0.000	1	50.0	4.477	4.478	0.027	0.001
1	35.3	4.539	4.553	0.017	0.014	1	45.0	4.448	4.481	0.024	0.033
1	30.0	4.510	4.544	0.018	0.034	1	40.0	4.424	4.484	0.022	0.060
						1	36.0	4.441	4.485	0.021	0.044
						1	32.0	4.438	4.486	0.025	0.048

References:
N=1 Mitchell and Yu (1980)
N=2 Souriau and Souriau (1983)

TABLE 11
VELOCITIES FOR 0-5 M.Y. OLD OCEANIC REGION
RAYLEIGH

N	T	C_o	C	±	$C-C_o$	N	T	U_o	U	±	$U-U_o$
	(s)	km/s	km/s	km/s	km/s		(s)	km/s	km/s	km/s	km/s
1	142.8	4.338	4.198	0.087	-0.140	1	137.0	3.476	3.605	0.095	0.129
1	125.0	4.131	4.116	0.041	-0.015	1	122.0	3.584	3.615	0.069	0.031
1	111.1	4.072	4.056	0.028	-0.017	1	107.5	3.643	3.624	0.041	-0.019
1	100.0	4.012	4.009	0.025	-0.003	1	94.3	3.613	3.632	0.041	0.019
1	90.9	3.967	3.974	0.022	0.007	1	83.3	3.625	3.642	0.028	0.017
1	77.0	3.925	3.921	0.017	-0.004	1	73.5	3.643	3.651	0.023	0.008
1	66.7	3.885	3.885	0.014	0.000	1	64.9	3.650	3.662	0.019	0.012
1	58.8	3.843	3.859	0.012	0.016	1	57.5	3.668	3.672	0.018	0.004
1	50.0	3.822	3.833	0.012	0.011	1	50.8	3.694	3.683	0.020	-0.011
1	40.0	3.803	3.807	0.013	0.004	1	44.6	3.729	3.695	0.023	-0.034
1	33.3	3.794	3.794	0.015	0.000	1	39.4	3.753	3.708	0.026	-0.045
1	25.0	3.784	3.786	0.016	0.002	1	34.8	3.756	3.724	0.027	-0.032
1	20.0	3.788	3.789	0.021	0.001	1	30.8	3.762	3.742	0.028	-0.020
1	16.7	3.771	3.792	0.027	0.021	1	27.1	3.769	3.762	0.028	-0.007
						1	23.9	3.774	3.782	0.031	0.008
						1	21.5	3.829	3.797	0.040	-0.032
						1	18.7	3.762	3.805	0.047	0.043
						1	16.4	3.828	3.813	0.077	-0.015

Reference: Forsyth (1975a)

TABLE 12
VELOCITIES FOR 5-10 M.Y. OLD OCEANIC REGION
RAYLEIGH

N	T	C_o	C	±	$C-C_o$	N	T	U_o	U	±	$U-U_o$
	(s)	km/s	km/s	km/s	km/s		(s)	km/s	km/s	km/s	km/s
1	142.8	4.174	4.200	0.100	0.026	1	137.0	3.493	3.600	0.132	0.107
1	125.0	4.044	4.117	0.062	0.073	1	122.0	3.568	3.615	0.108	0.047
1	111.1	3.999	4.056	0.043	0.057	1	107.5	3.753	3.629	0.075	-0.124
1	100.0	3.961	4.011	0.041	0.050	1	94.3	3.672	3.646	0.075	-0.026
1	90.9	3.975	3.976	0.038	0.001	1	83.3	3.646	3.666	0.047	0.020
1	77.0	3.930	3.927	0.028	-0.003	1	73.5	3.636	3.685	0.038	0.049
1	66.7	3.890	3.896	0.025	0.006	1	64.9	3.690	3.707	0.033	0.017
1	58.8	3.862	3.875	0.021	0.013	1	57.5	3.723	3.730	0.031	0.007
1	50.0	3.846	3.856	0.021	0.010	1	50.8	3.793	3.754	0.034	-0.039
1	40.0	3.848	3.844	0.022	-0.004	1	44.6	3.810	3.782	0.039	-0.027
1	33.3	3.852	3.845	0.025	-0.007	1	39.4	3.827	3.814	0.045	-0.013
1	25.0	3.886	3.863	0.031	-0.023	1	34.8	3.885	3.849	0.049	-0.036
1	20.0	3.903	3.887	0.036	-0.017	1	30.8	3.992	3.886	0.051	-0.106
1	16.7	3.888	3.898	0.043	0.010	1	27.1	3.925	3.925	0.052	0.000
						1	23.9	3.875	3.967	0.054	0.086
						1	21.5	3.752	3.983	0.062	0.231
						1	18.7	3.694	3.993	0.074	0.299
						1	16.4	3.830	4.005	0.103	0.175

Reference: Forsyth (1975a)

TABLE 13
VELOCITIES FOR 10-20 M.Y. OLD OCEANIC REGION
RAYLEIGH

N	T	C_o	C	±	$C-C_o$	N	T	U_o	U	±	$U-U_o$
	(s)	km/s	km/s	km/s	km/s		(s)	km/s	km/s	km/s	km/s
1	142.8	4.242	4.232	0.056	-0.010	1	137.0	3.658	3.640	0.070	-0.018
1	125.0	4.205	4.150	0.062	-0.055	1	122.0	3.618	3.660	0.045	0.042
1	111.1	4.120	4.092	0.018	-0.028	1	107.5	3.626	3.682	0.029	0.056
1	100.0	4.069	4.049	0.017	-0.020	1	94.3	3.674	3.706	0.030	0.032
1	90.9	4.029	4.017	0.015	-0.013	1	83.3	3.726	3.732	0.021	0.006
1	77.0	3.971	3.973	0.012	0.002	1	73.5	3.747	3.756	0.018	0.009
1	66.7	3.938	3.946	0.011	0.008	1	64.9	3.777	3.784	0.015	0.007
1	58.8	3.924	3.928	0.009	0.004	1	57.5	3.812	3.811	0.014	-0.001
1	50.0	3.914	3.915	0.009	0.001	1	50.8	3.841	3.840	0.015	-0.001
1	40.0	3.911	3.910	0.010	-0.001	1	44.6	3.885	3.872	0.018	-0.013
1	33.3	3.920	3.916	0.011	-0.004	1	39.4	3.923	3.906	0.021	-0.018
1	25.0	3.938	3.939	0.014	0.001	1	34.8	3.950	3.941	0.022	-0.009
1	20.0	3.948	3.961	0.017	0.012	1	30.8	3.971	3.976	0.023	0.005
						1	27.1	3.962	4.010	0.023	0.048
						1	23.9	3.951	4.033	0.025	0.082
						1	21.5	3.935	4.041	0.030	0.106
						1	18.7	3.881	4.035	0.035	0.154
						1	16.4	3.661	4.015	0.042	0.354

Reference: Forsyth (1975a)

TABLE 14
VELOCITIES FOR 0-10 M.Y. OLD OCEANIC REGION
RAYLEIGH

N	T	C_o	C	±	$C-C_o$	N	T	U_o	U	±	$U-U_o$
	(s)	km/s	km/s	km/s	km/s		(s)	km/s	km/s	km/s	km/s
1	142.6	4.287	4.200	0.081	-0.087	1	137.0	3.477	3.596	0.087	0.119
1	125.0	4.098	4.117	0.037	0.019	1	122.0	3.590	3.606	0.061	0.016
1	111.1	4.049	4.055	0.025	0.006	1	107.5	3.675	3.614	0.038	-0.061
1	100.0	3.999	4.007	0.021	0.008	1	94.3	3.628	3.623	0.035	-0.005
1	90.9	3.969	3.971	0.018	0.002	1	83.3	3.628	3.634	0.024	0.006
1	77.0	3.924	3.917	0.014	-0.007	1	73.5	3.636	3.644	0.019	0.008
1	66.7	3.883	3.881	0.012	-0.003	1	64.9	3.657	3.656	0.016	-0.001
1	58.8	3.844	3.854	0.010	0.010	1	57.5	3.678	3.667	0.016	-0.011
1	50.0	3.824	3.828	0.010	0.004	1	50.8	3.713	3.679	0.018	-0.034
1	40.0	3.810	3.803	0.011	-0.007	1	44.6	3.745	3.694	0.019	-0.051
1	33.3	3.805	3.791	0.012	-0.014	1	39.4	3.768	3.710	0.021	-0.058
1	25.0	3.808	3.789	0.015	-0.019	1	34.8	3.788	3.731	0.023	-0.057
1	20.0	3.819	3.800	0.018	-0.019	1	30.8	3.806	3.755	0.024	-0.051
1	16.7	3.813	3.807	0.021	-0.006	1	27.1	3.812	3.785	0.024	-0.027
						1	23.9	3.804	3.815	0.025	0.011
						1	21.5	3.811	3.839	0.032	0.028
						1	18.7	3.746	3.855	0.039	0.109
						1	16.4	3.797	3.874	0.057	0.077

Reference: Forsyth (1975a)

TABLE 15
Uppermantle velocities for each Mitchell and Yu age province

thicknesses	0-20	20-50	A	B	50-100	>100
water	3.45	4.67	5.05	4.85	5.40	5.75
sediment	0.02	0.13	0.18	0.18	0.23	0.30
crust 1	1.51	1.58	1.60	1.60	1.60	1.60
crust 2	4.84	5.15	5.19	5.19	5.19	5.19
lid 1	6.00	6.00	6.00	6.00	6.00	6.00
lid 2	14.00	24.00	29.00	34.00	34.00	44.00
	VPV	VPH	VSV	VSH	ETA	Q_μ
	km/s	km/s	km/s	km/s		
water	1.52	1.52	0.00	0.00	1.00	∞
sediment	1.65	1.65	1.00	1.00	1.00	600
LID 1	8.02	8.19	4.40	4.61	0.90	600
crust 1						
0-20, 20-50	5.21	5.21	3.03	3.03	1.00	600
B	5.15	5.15	3.00	3.00	1.00	600
A	4.94	4.94	2.88	2.88	1.00	600
50-100	5.07	5.07	2.96	2.96	1.00	600
>100	5.01	5.01	2.93	2.93	1.00	600
crust 2						
0-20, 20-50, B	6.80	6.80	3.90	3.90	1.00	600
A	6.53	6.53	3.74	3.74	1.00	600
50-100	6.70	6.70	3.84	3.84	1.00	600
>100	6.63	6.63	3.80	3.80	1.00	600
LID 2						
0-20	8.21	8.21	4.60	4.60	1.00	600
20-50	8.42	8.42	4.72	4.72	1.00	600
A, B	8.41	8.41	4.71	4.71	1.00	600
50-100	8.39	8.48	4.70	4.75	1.00	600
>100	8.27	8.31	4.63	4.66	1.00	600
LVZ top						
0-20	7.67	7.90	4.20	4.45	0.92	80
20-50	7.77	7.88	4.28	4.39	0.93	80
B	7.48	8.00	4.36	4.51	0.83	80
A	7.92	8.02	4.36	4.49	0.88	80
50-100	8.04	8.15	4.43	4.58	0.83	80
>100	8.12	8.12	4.48	4.56	0.87	80
LVZ bottom						
0-20	7.57	7.77	4.31	4.28	1.00	80
20-50	7.59	7.77	4.32	4.29	1.00	80
B	7.53	8.05	4.43	4.37	1.01	80
A	7.52	7.87	4.28	4.36	0.98	80
50-100	7.46	8.03	4.25	4.43	0.96	80
>100	7.66	8.03	4.36	4.31	0.97	80
220						
0-20, 20-50	8.47	8.47	4.60	4.60	1.00	143
A, B, 50-100, >100	8.56	8.56	4.64	4.64	1.00	143
400						
0-20, 20-50	8.82	8.82	4.72	4.72	1.00	143
A, B, 50-100, >100	8.91	8.91	4.77	4.77	1.00	143

TABLE 16
Uppermantle Velocities for each Forsyth oceanic province

Thicknesses	0-5	5-10	10-20	0-10
water	3.10	3.40	3.75	3.10
sediment	0.00	0.00	0.15	0.00
crust 1	1.51	1.51	1.51	1.51
crust 2	4.64	4.64	4.64	4.64
LID 1	6.00	6.00	6.00	6.00
LID 2	10.00	16.00	20.00	10.00

all provinces

	VPV	VPH	VSV	VSH	ETA	Q_μ
	km/s	km/s	km/s	km/s		
water	1.52	1.52	0.00	0.00	1.00	∞
sediment	1.65	1.65	1.00	1.00	1.00	600
crust 1	5.21	5.21	3.03	3.03	1.00	600
crust 2	6.80	6.80	3.90	3.90	1.00	600
LID 1	8.02	8.19	4.40	4.61	0.90	600
220	8.47	8.47	4.60	4.60	1.00	143
400	8.82	8.82	4.72	4.72	1.00	143
LID 2						
0-5	8.00	8.00	4.48	4.48	1.00	600
5-10	8.40	8.40	4.70	4.70	1.00	600
10-20	8.43	8.43	4.75	4.75	1.00	600
0-10	8.30	8.30	4.65	4.65	1.00	600
LVZ top						
0-5	7.43	7.68	4.07	4.32	0.92	80
5-10	7.48	7.68	4.10	4.32	0.93	80
10-20	7.63	7.88	4.19	4.44	0.92	80
0-10	7.45	7.78	4.09	4.41	0.93	80
LVZ bottom						
0-5	7.67	7.39	4.37	4.08	1.01	80
5-10	7.59	7.41	4.32	4.09	1.01	80
10-20	7.66	7.75	4.36	4.27	1.00	80
0-10	7.67	7.50	4.37	4.06	1.01	80

TABLE 17
Upper mantle velocities for the average Earth model

	Thickness	VPV	VPH	VSV	VSH	ETA	Q_μ
	km	km/s	km/s	km/s	km/s		
water	3.00	1.45	1.45	0.00	0.00	1.00	∞
crust1	12.00	5.80	5.80	3.20	3.20	1.00	600
crust2	3.40	6.80	6.80	3.90	3.90	1.00	600
LID	28.42	8.02	8.19	4.40	4.61	.90	600
LVZ top		7.90	8.00	4.36	4.58	.80	80
LVZ bottom		7.95	8.05	4.43	4.44	.98	80
220		8.56	8.56	4.64	4.64	1.00	143
400		8.91	8.91	4.77	4.77	1.00	143

TABLE 18
Comparison of two average ocean models

	all		<150		>150	
	SW	S	SW	S	SW	S
Model 1						
c_R	11.55	8.238	2.449	2.630	12.44	8.762
u_R	26.92	33.98	35.51	35.37	17.64	27.86
c_L	11.40	10.90	13.51	16.87	3.63	3.86
u_L	18.51	22.43	18.51	22.43		
Model 2						
c_R	10.70	7.257	6.340	6.327	10.47	7.449
u_R	21.58	26.73	26.98	28.94	15.18	24.65
c_L	11.95	14.99	15.71	17.51	3.681	4.010
u_L	18.49	22.42	18.49	22.42		
Totals						
Model 1	24.15	24.72	28.10	28.50	14.75	19.01
Model 2	18.79	21.29	25.37	24.54	10.99	16.55

FIGURE CAPTIONS

Figure.1: Phase velocity dispersion curves for the average Earth. Lower curve is for Rayleigh waves, Upper curve is for Love waves. Data points are indicated by +. Where no error bars are visible standard deviations are less than or equal to the width of the horizontal bar of the +. Solid lines give the best fitting average Earth model.

Figure.2: Group velocity dispersion curves for the average Earth. Symbols as in figure 1

Figure.3: Phase and group velocity dispersion curves for the average ocean. Lower curve in each plot is for Rayleigh waves, upper curve is for Love waves. Where no error bars are visible the standard deviations are about half the width of the point for phase velocity, and the order of the line thickness for group velocity. The solid lines give the dispersion calculated for average ocean model A.

Figure.4: Same as figure 3 but the solid lines give the dispersion calculated for average ocean model B.

Figure.5: Phase and group velocity dispersion curves for Mitchell and Yu's 0-20 M.Y. old oceanic province are given in the leftmost two plots. Corresponding plots for their 20-50 M.Y. old oceanic province are given in the rightmost two plots. Details of are the same as for figure 3.

Figure.6: Phase and group velocity dispersion for Mitchell and Yu's 50-100 M.Y. old oceanic province are given in the leftmost two plots. Corresponding plots for their >100 M.Y. old oceanic province are given in the rightmost two plots. Details are the same as for figure 3.

Figure.7: Phase and group velocity dispersion for Forsyth's 0-5 M.Y. old oceanic province are given in the rightmost pair of plots. Corresponding plots for 5-10 M.Y. old oceanic province are given in the leftmost pair of plots. Details are the same as for figure 3.

Figure.8: Phase and group velocity dispersion for Forsyth's 10-20 M.Y. old oceanic province are given in the rightmost pair of plots. Corresponding plots for his 0-10 M.Y. old oceanic age province are given in the leftmost pair of plots. Details of each plot are the same as for figure 3.

Figure.9: Changes in Rayleigh wave phase velocity dispersion curves caused by changes in each of the parameters varied in the study. Except where otherwise noted changes are in the LVZ. From right to left the parameters changed are the following; TOP ROW: SH velocity gradient(SHG), mean SH velocity (SHM), ETA gradient (ETAG), mean ETA (ETAM), lid thickness (THL). MIDDLE ROW: SH and PH velocity in the lid with SH/PH constant (LH), mean PH velocity (PHM), PV velocity gradient (PVG), PH velocity gradient (PHG), SV velocity gradient (SVG). BOTTOM ROW: mean PV velocity (PVM), crustal velocity (VCR), crustal thickness (THCR), SV and PV velocity in the lid with SV/PV constant (LV), mean SV velocity(SVM). Horizontal scale is

from 0s to 300s

Figure.10: Changes to Rayleigh wave group velocity dispersion curves due to changes in each of the parameters varied in this study. The parameters are displayed in the same order as figure 9.

Figure.11: Changes in Love wave phase velocity dispersion curves due to changes in each of the parameters varied in this study. Except where otherwise indicated changes are in the LVZ.

From right to left the parameters changes are the following; TOP ROW:PVM, PVG, ETAM, ETAG, PHG. MIDDLE ROW: LV, SVM, SHG, SVG, THL. BOTTOM ROW: SHM, VCR, THCR, LH, PHM.

Codes used are those in the caption of figure 9. Horizontal scale is 0s - 300s.

Figure.12: Changes in Love wave group velocity dispersion curves due to changes in each of the parameters varied in this study. The parameters are displayed in the same order as figure 11.

Figure.13: Velocity depth profiles for two average ocean models that fit the data equally well. Dispersion curves for model A (solid lines) are shown in figure 3. Dispersion curves for model B (dashed lines) are shown in figure 4. From left to right the top row gives SV, PV, and ETA and the bottom row gives SH, and PH.

Figure.14: Rayleigh wave phase and group velocity residuals for the two average ocean models. Upper right plot shows model B group velocity residuals, lower right shows model B phase velocity residuals. Upper left plot shows model A group velocity residuals and lower left shows model A phase velocity residuals. A positive residual indicates that the model is too fast.

Figure.15: Love wave phase and group velocity residuals for the two average ocean models. Layout is the same as figure 14.

Figure.16: Velocity depth profiles for the average Earth model. From left to right solid lines show PV, SV, and ETA, and dotted lines show PH, and SH. Dispersion curves for this model are shown in figures 1 and 2.

Figure.17: Velocity depth profiles for the 0-20 M.Y. (upper set) and the 20-50 M.Y. (lower set) old age provinces of Mitchell and Yu. Details of each set are the same as figure 16. Corresponding dispersion curves are given in figure 5.

Figure.18: Velocity depth profiles for the 50-100 M.Y. (upper set) and the >100 M.Y. (lower set) old oceanic regions of Mitchell and Yu. Details of each set are the same as figure 16. Corresponding dispersion curves are shown in figure 6.

Figure.19: Velocity depth profiles for the 0-5 M.Y. (upper set) and the 5-10 M.Y. (lower set) old oceanic regions of Forsyth. Details of each set are the same as in figure 16. Corresponding dispersion curves are shown in figure 7.

Figure.20: Velocity depth profiles for the 10-20 M.Y. (upper set) and the 0-10 M.Y. (lower set) old oceanic regions of Forsyth. Details of each set are the same as in figure 16. Corresponding dispersion curves are shown in figure 8.

Figure.21: The thickness of the seismic lithosphere as determined in this study. The upper edge of the open boxes gives the thickness of the LID only. The lower edge gives the thickness of the LID plus the crust. The elastic thicknesses and the isotherms are from Watts et. al. [1980]. The triangle is a refraction measurement of lithosphere thickness from Nagumo et. al. [1981].

Figure.22: Schematic representation of seismic velocities due to temperature, pressure, and crystal orientation assuming a flow aligned olivine model. The upper left diagram shows a convection cell with arrows indicating flow direction. The trench is indicated by T, the ridge by R, and the midpoint by M. The lower left diagram shows temperature depth profiles for the trench, ridge, and midpoint. The upper and lower right diagrams show the nature of the velocity depth structure of VSH and VSV respectively due to pressure, temperature, and crystal orientation.

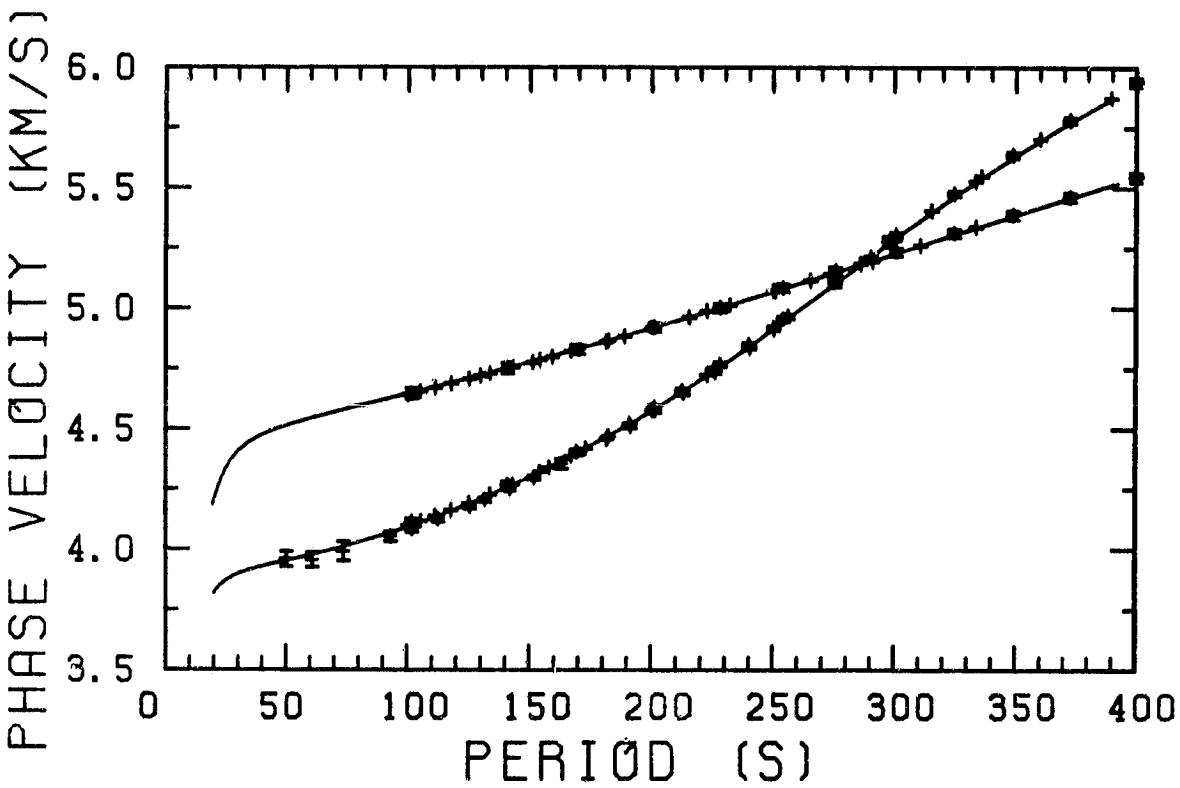

Fig. 1

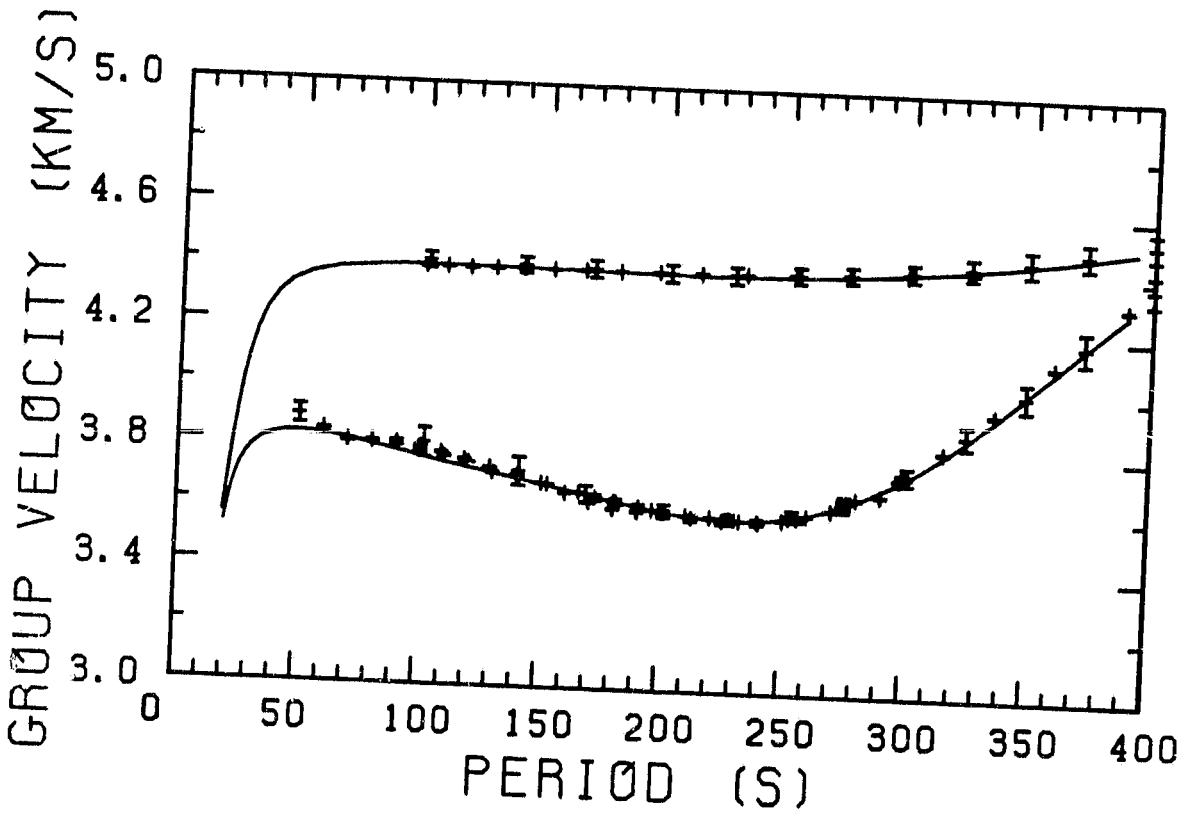

Fig. 2

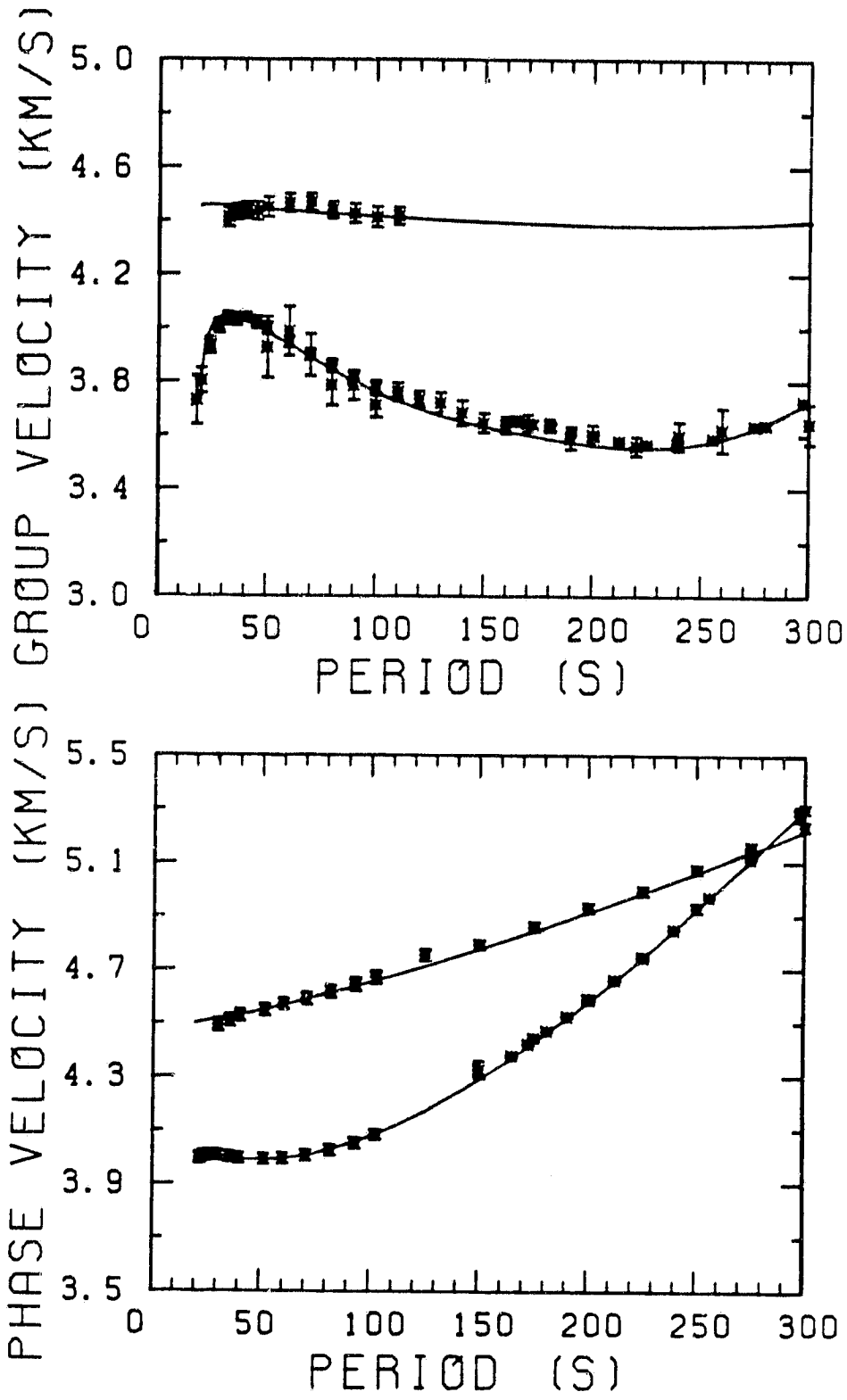

Fig. 3

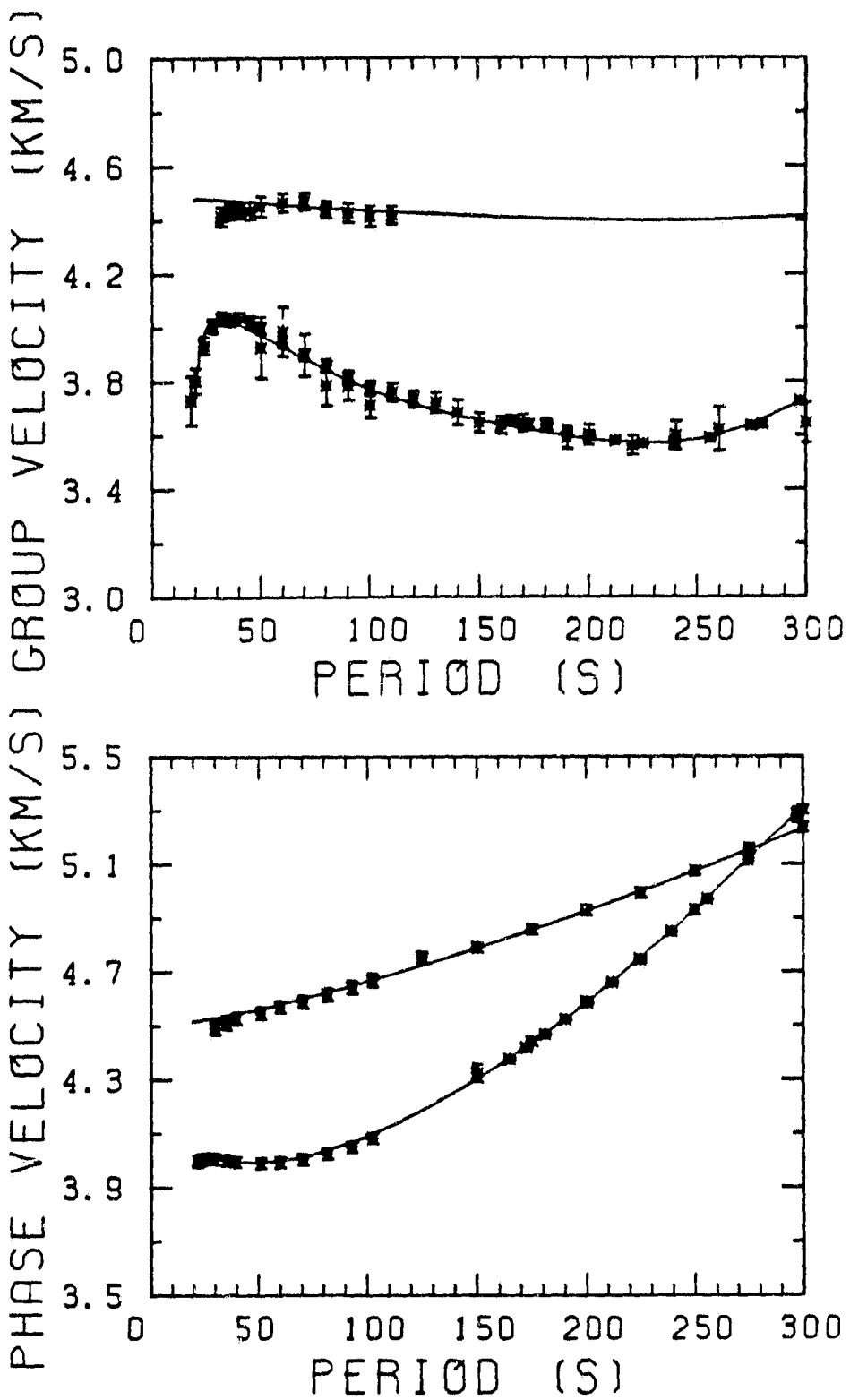

Fig. 4

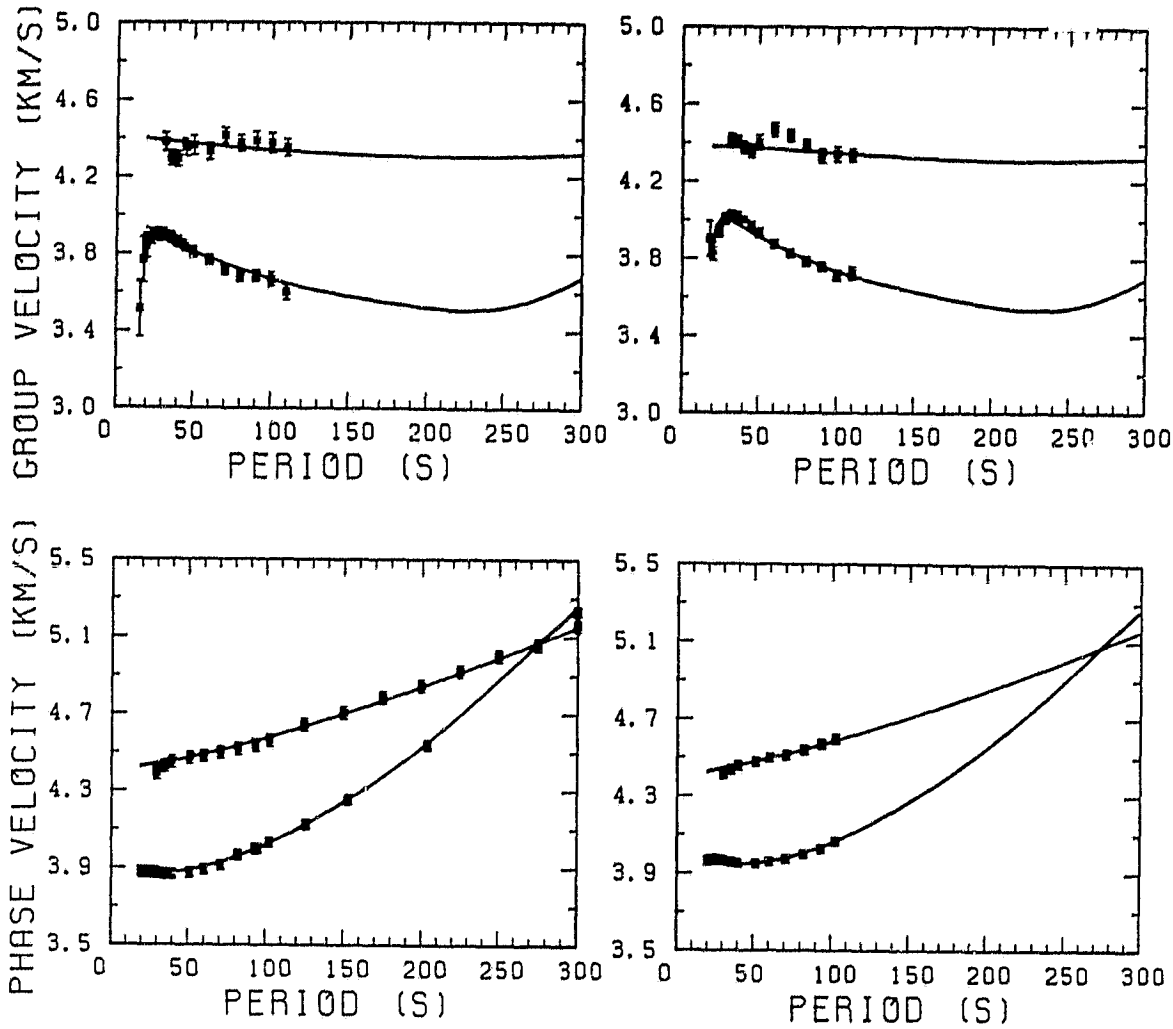

Fig. 5

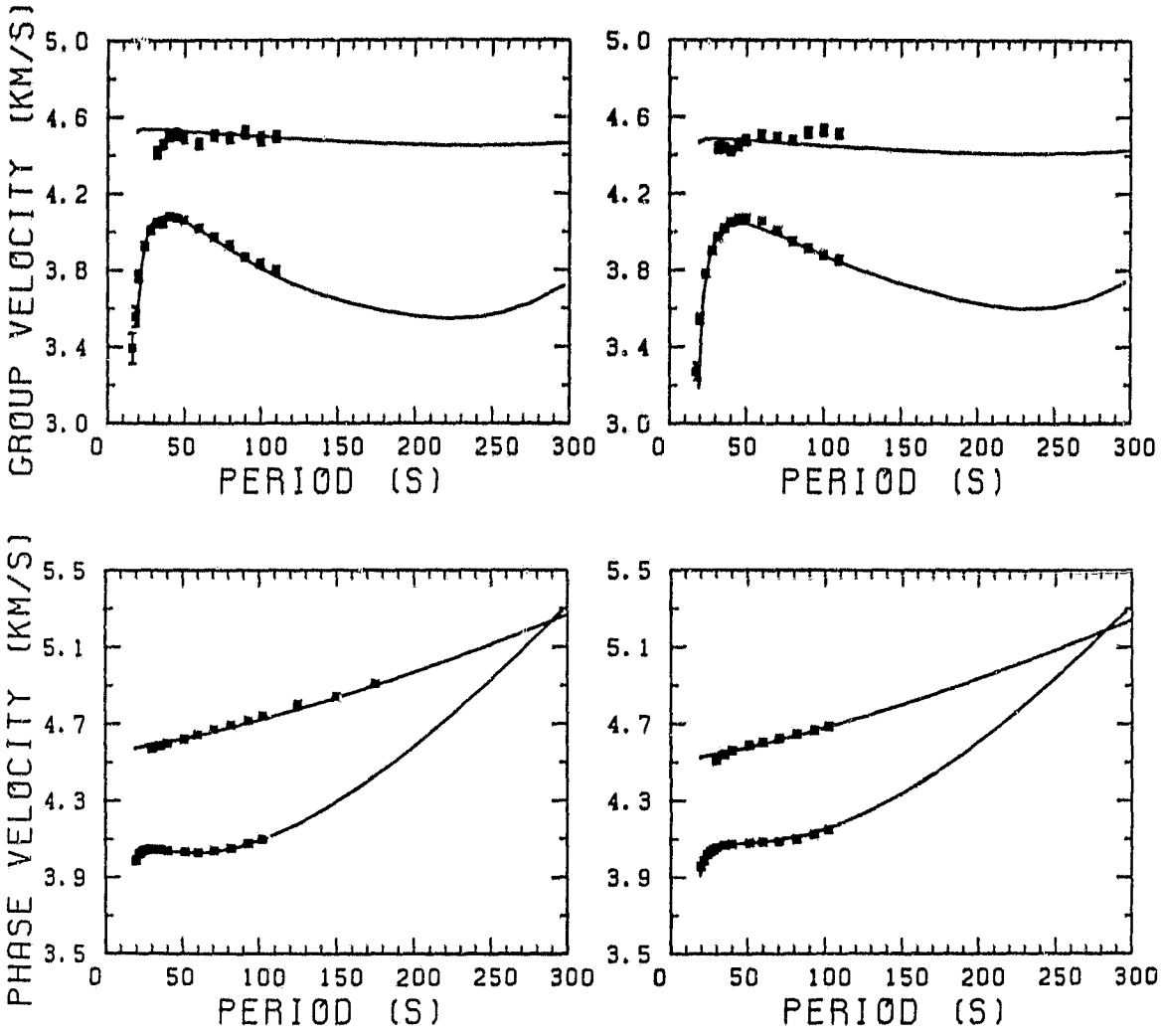

Fig. 6

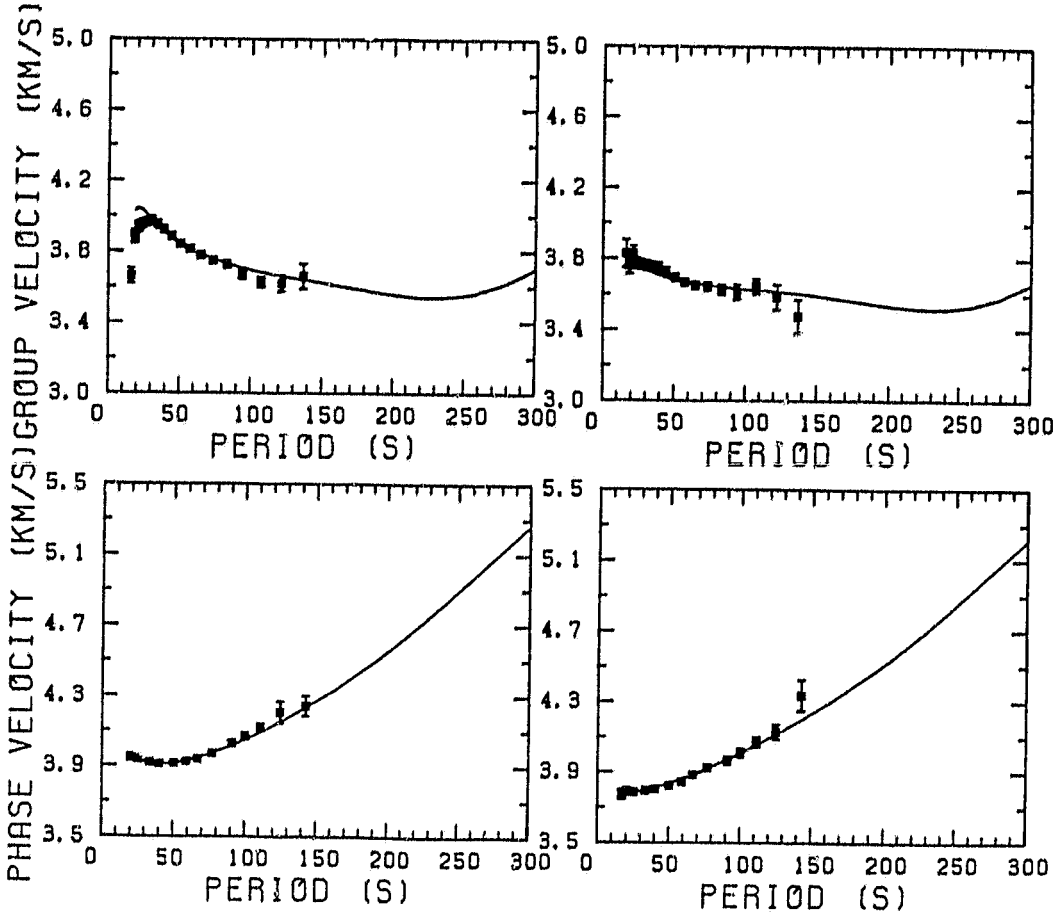

Fig. 7

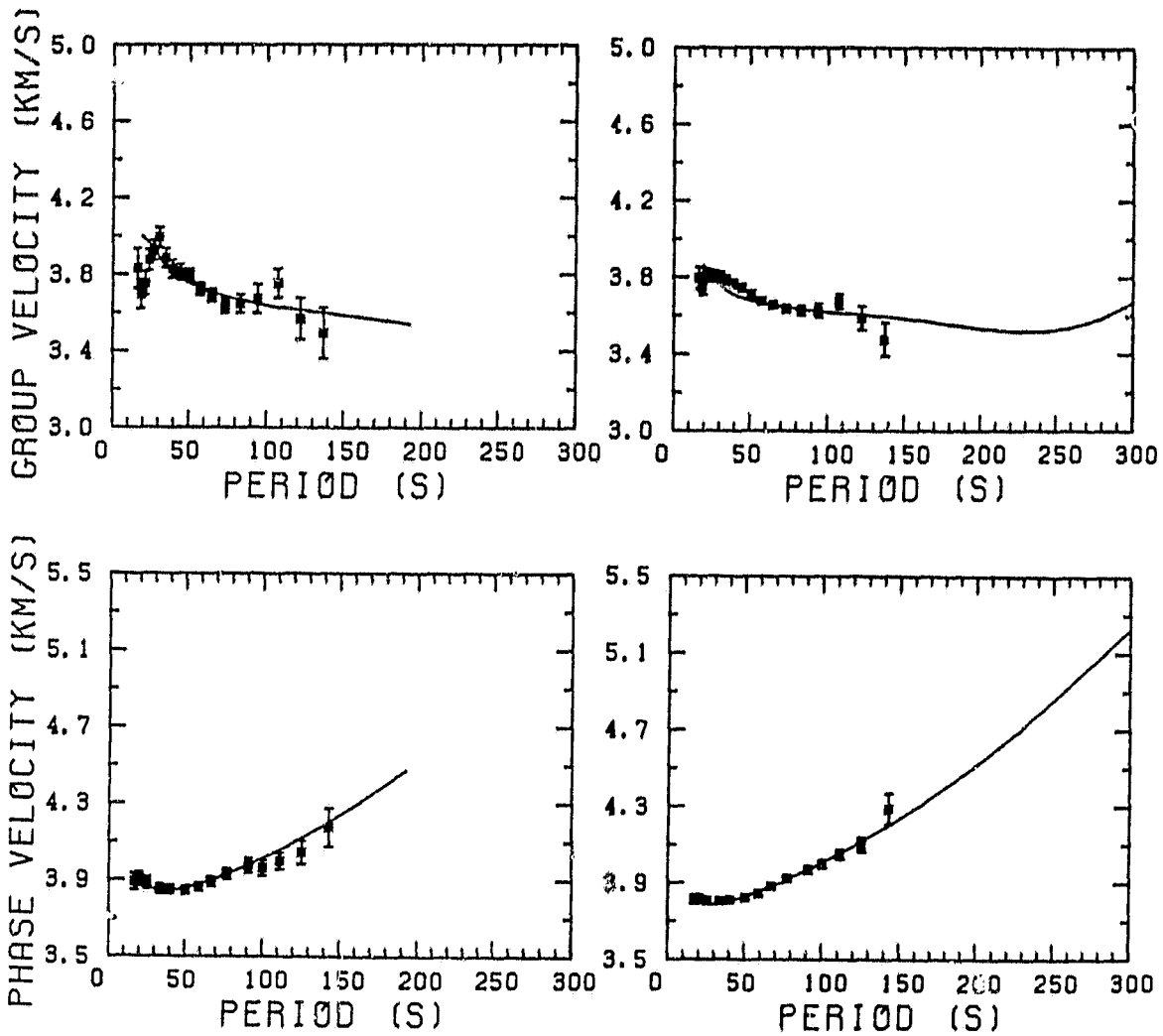

Fig. 8

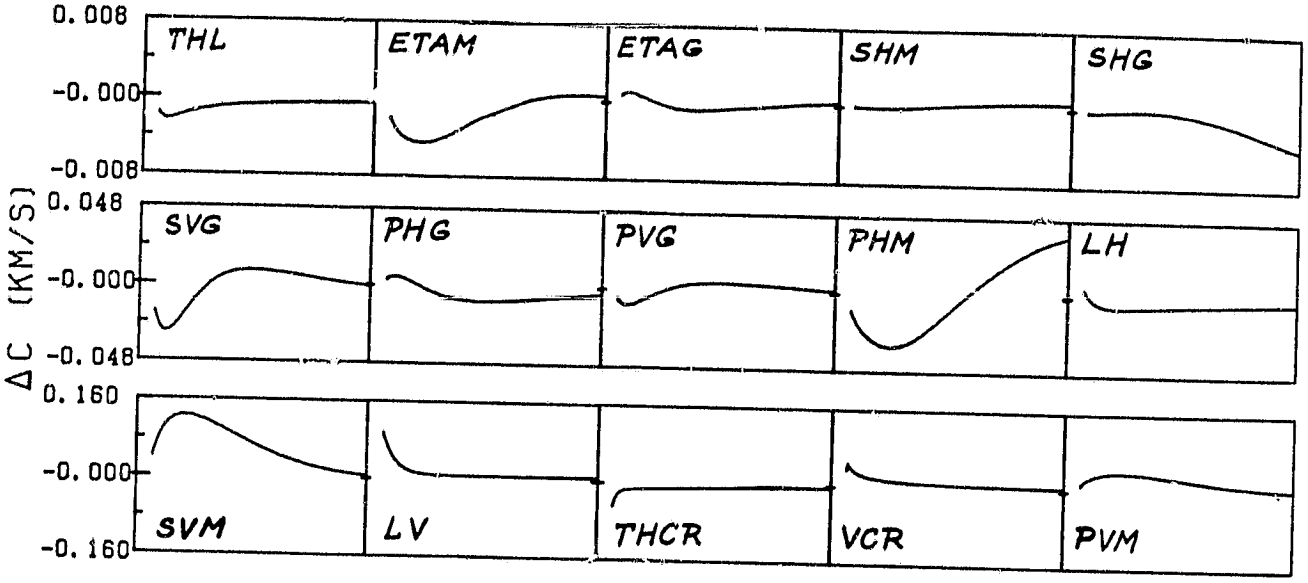

Fig. 9

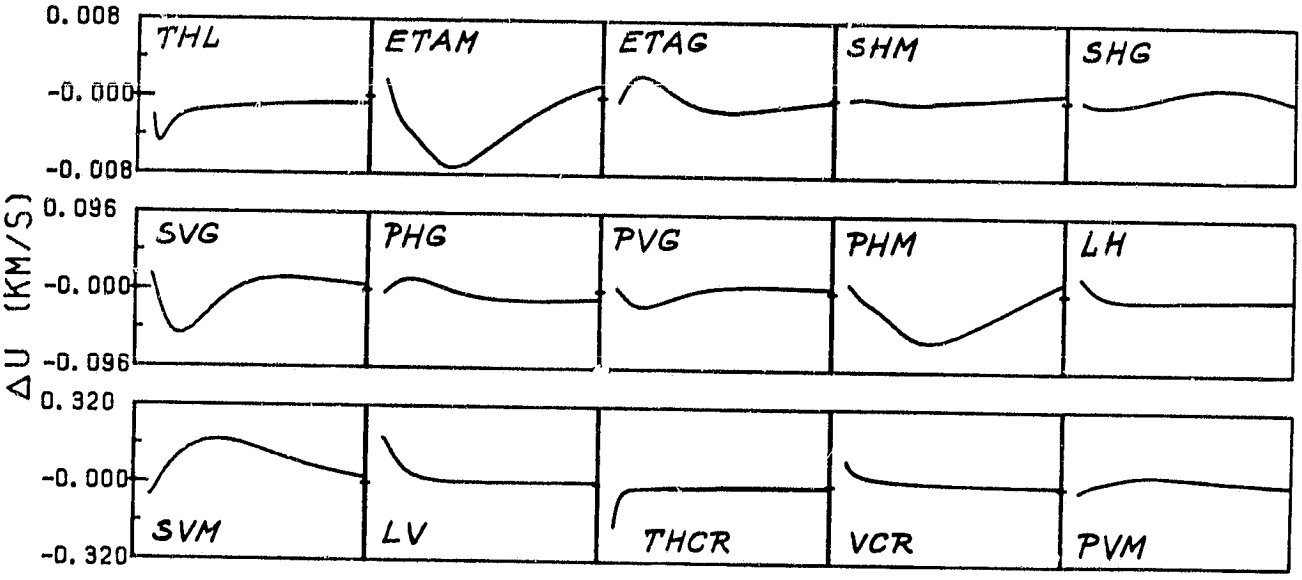

Fig. 10

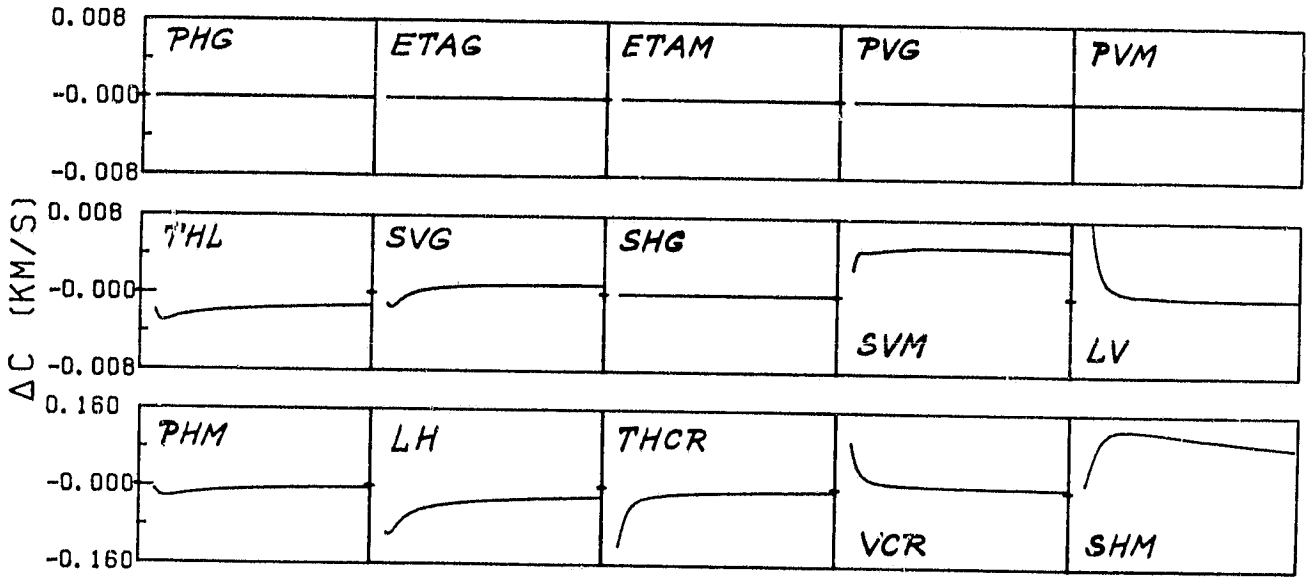

Fig. 11

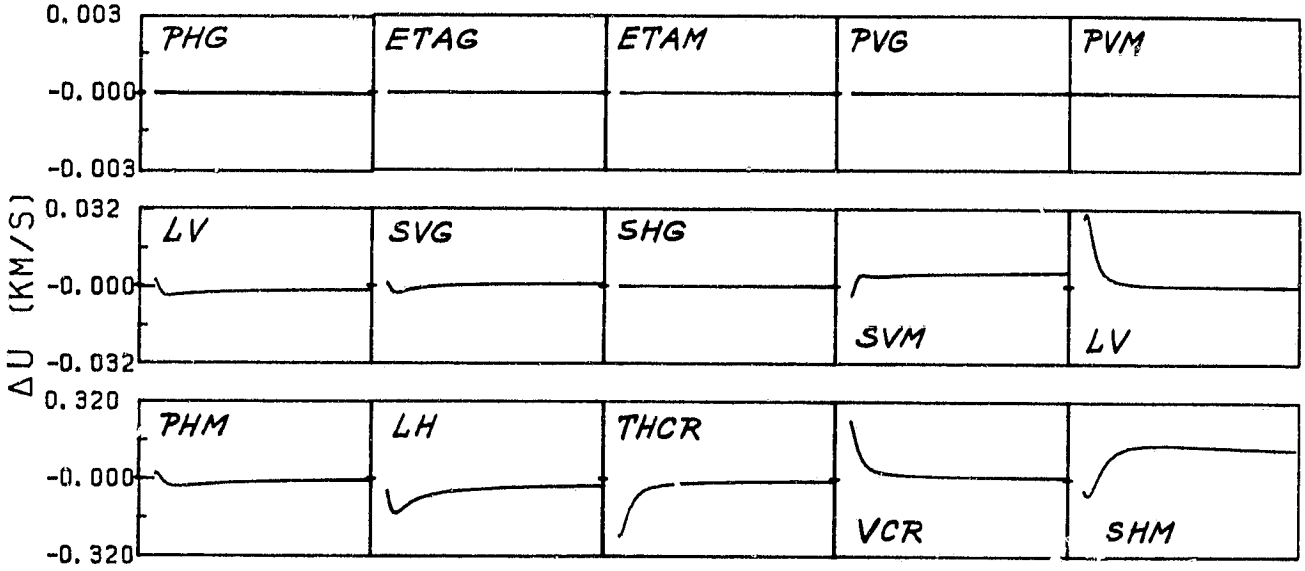

Fig. 12

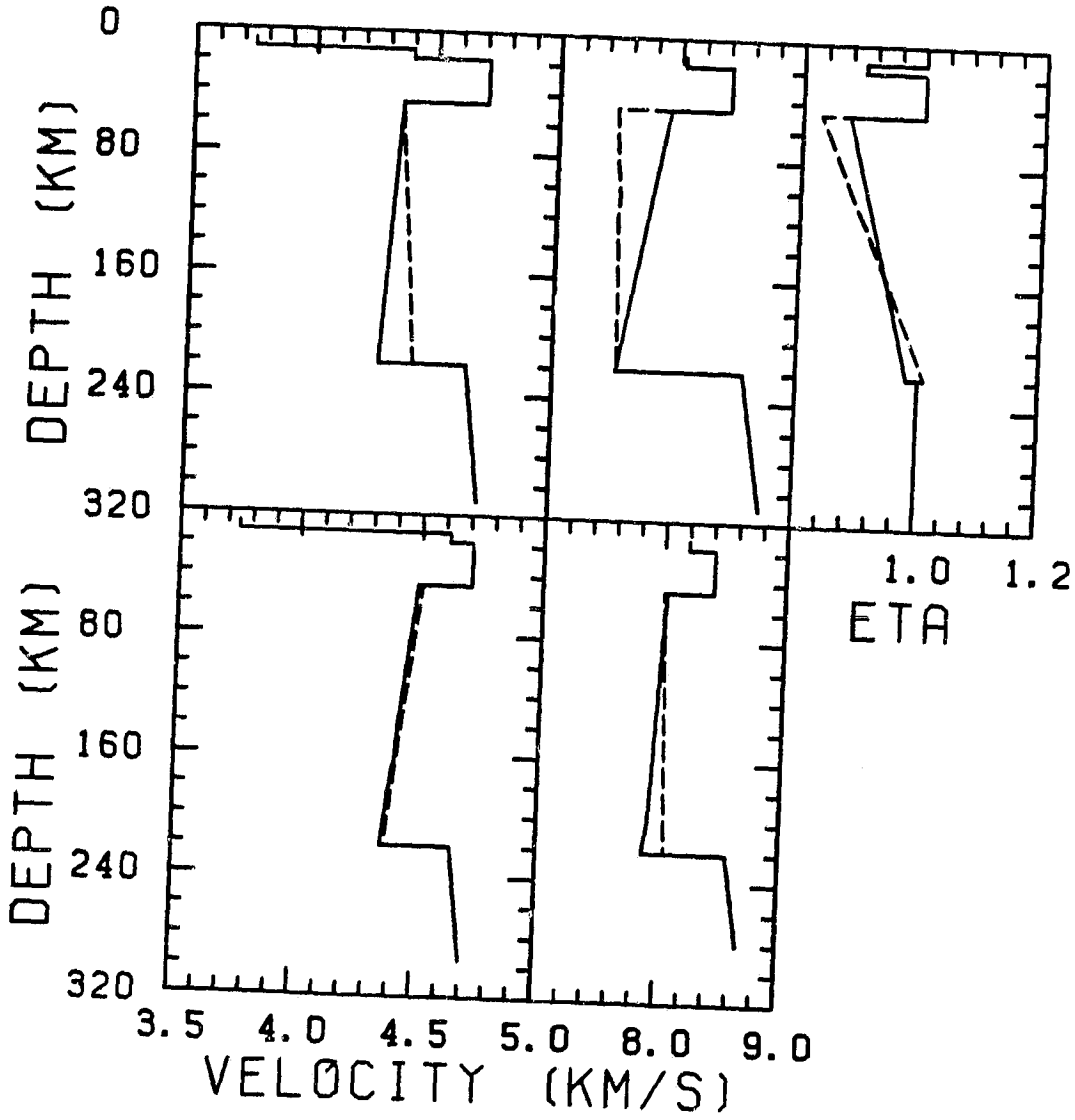

Fig. 13

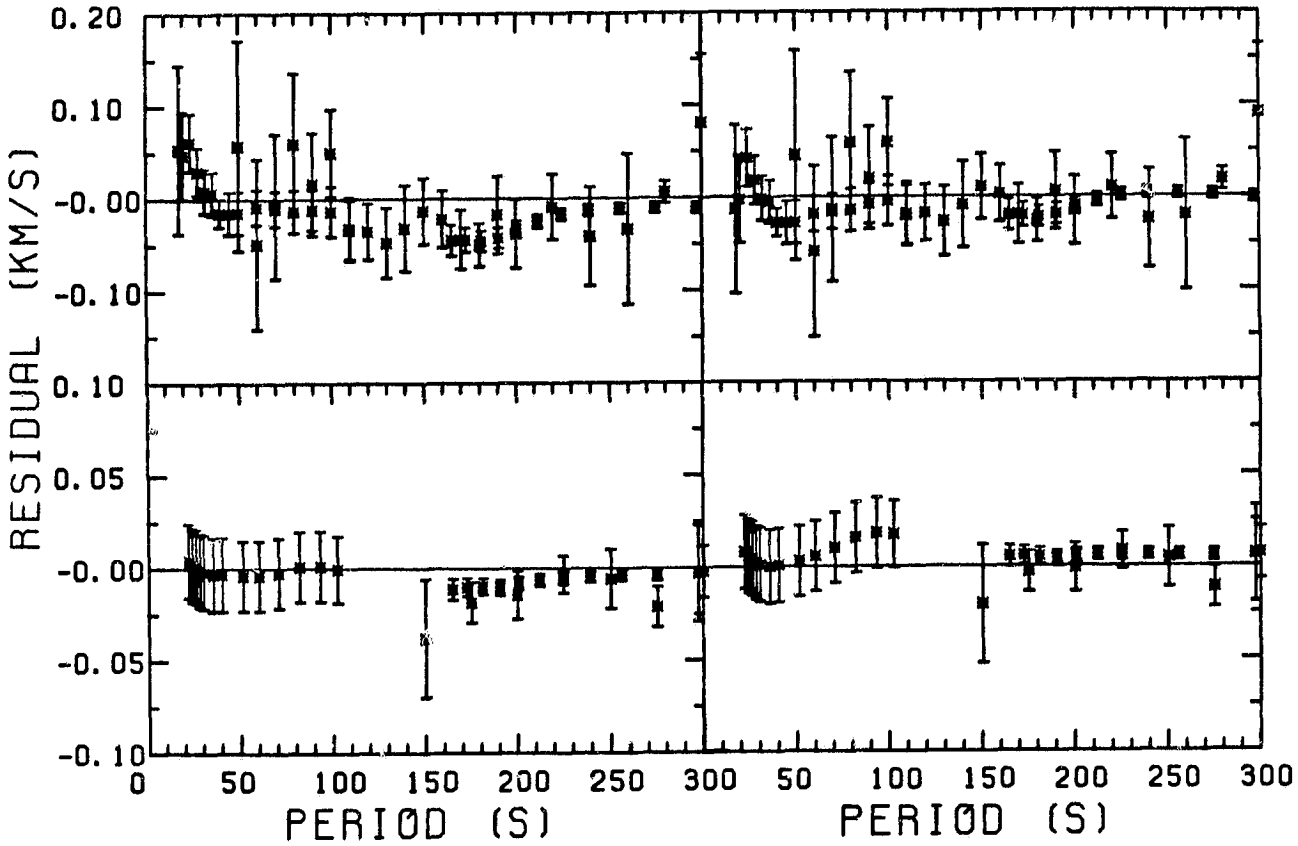

Fig. 14

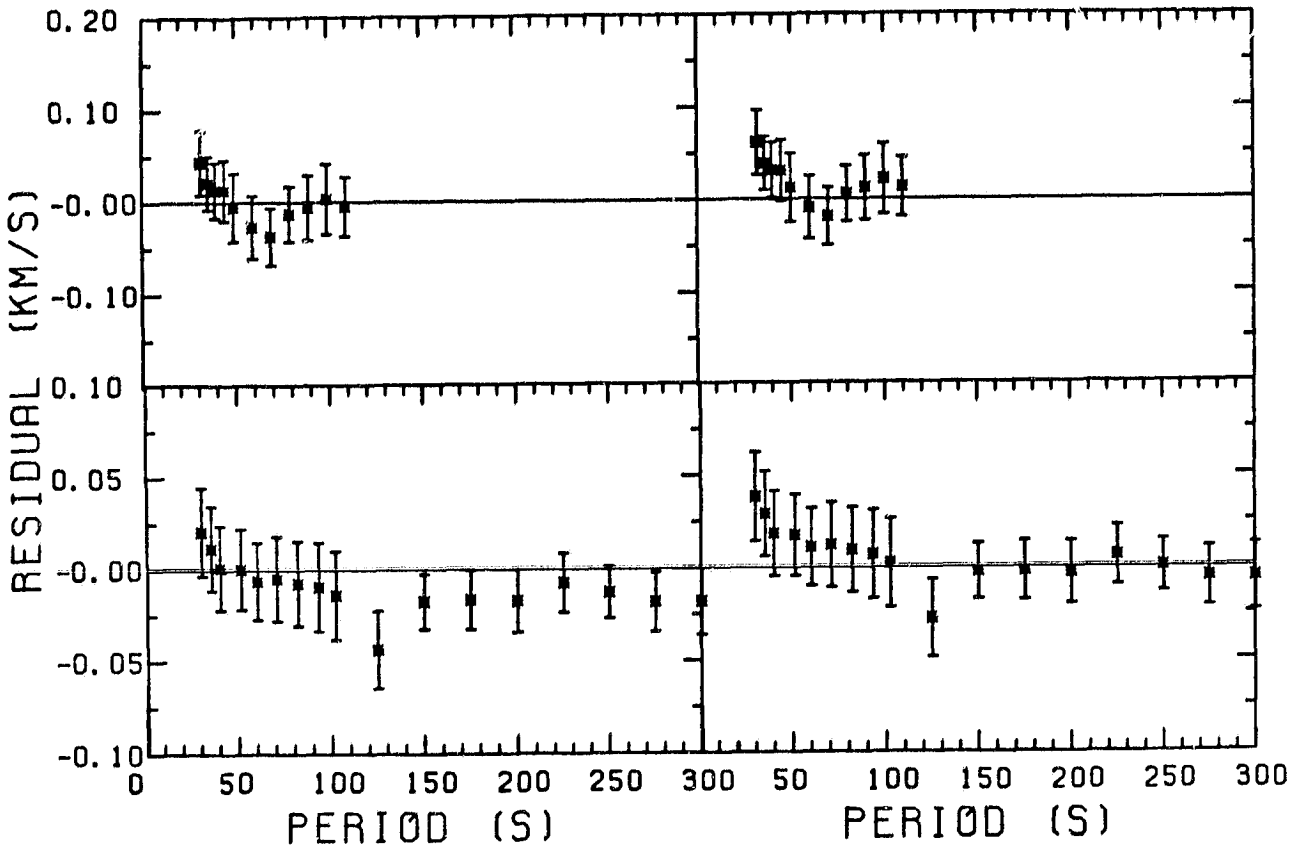

Fig. 15

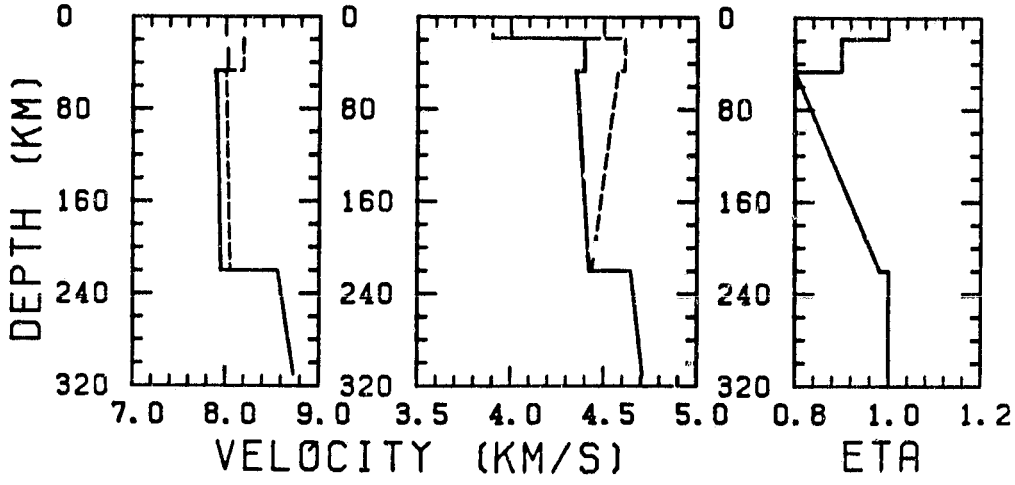

Fig. 16

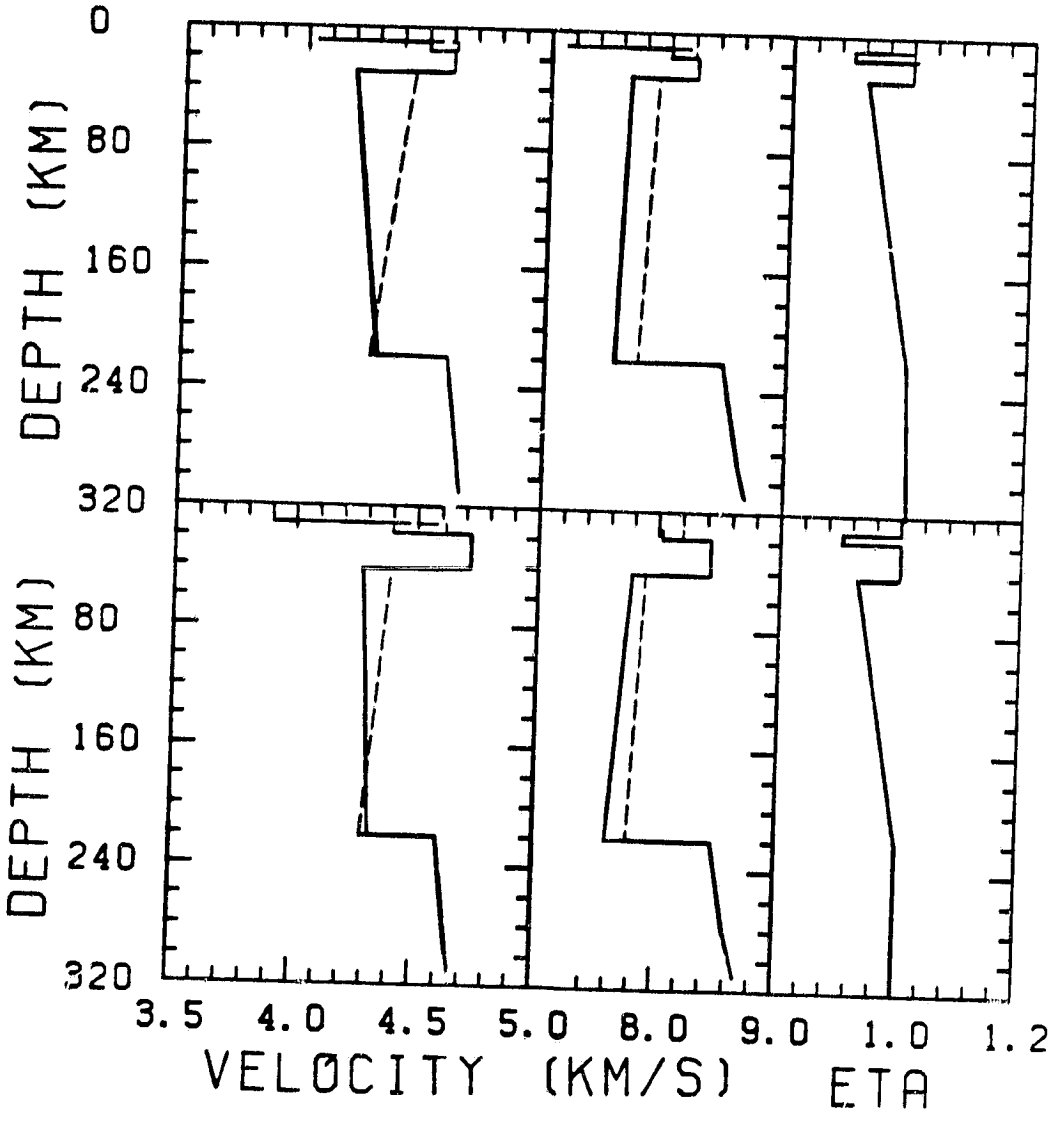

Fig. 17

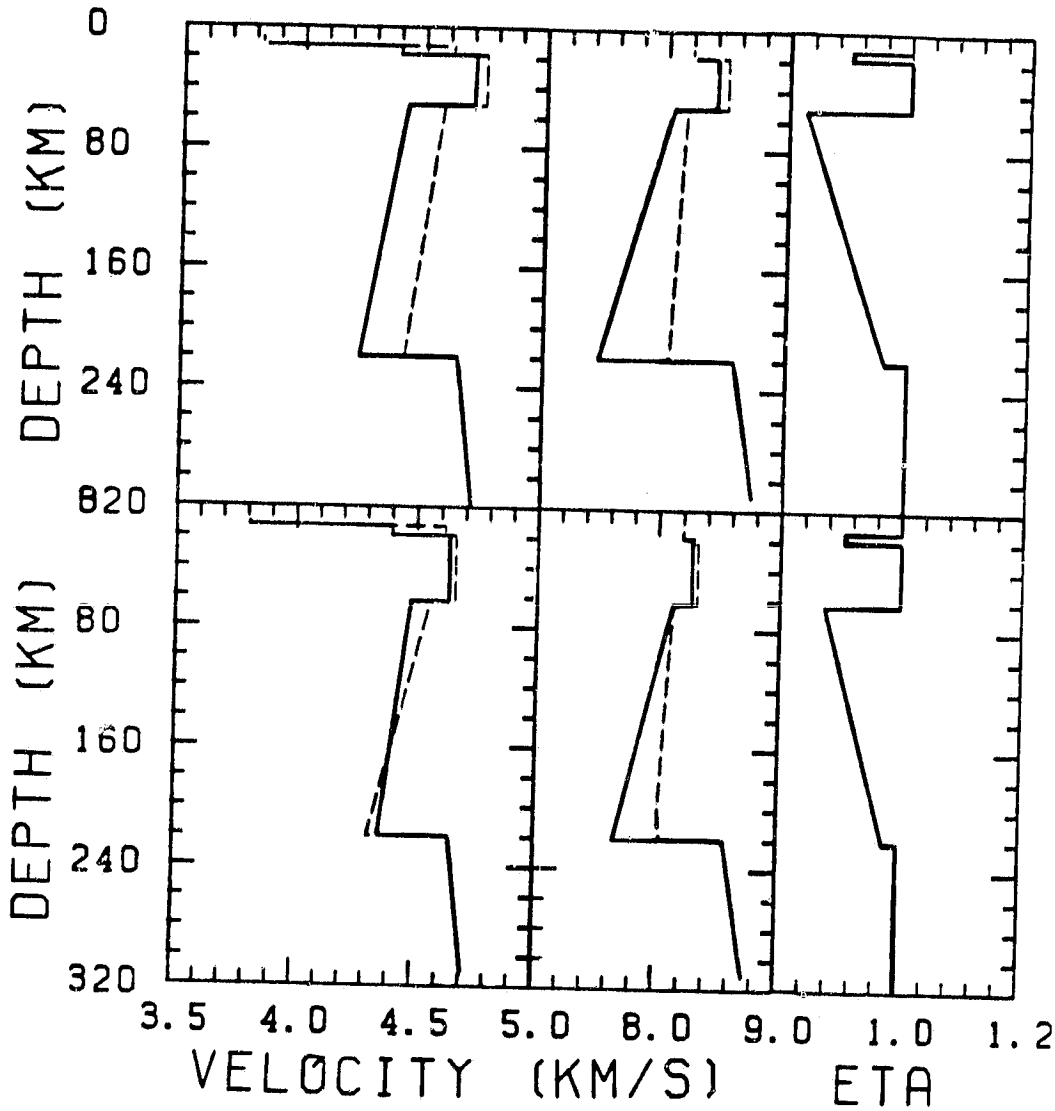

Fig. 18

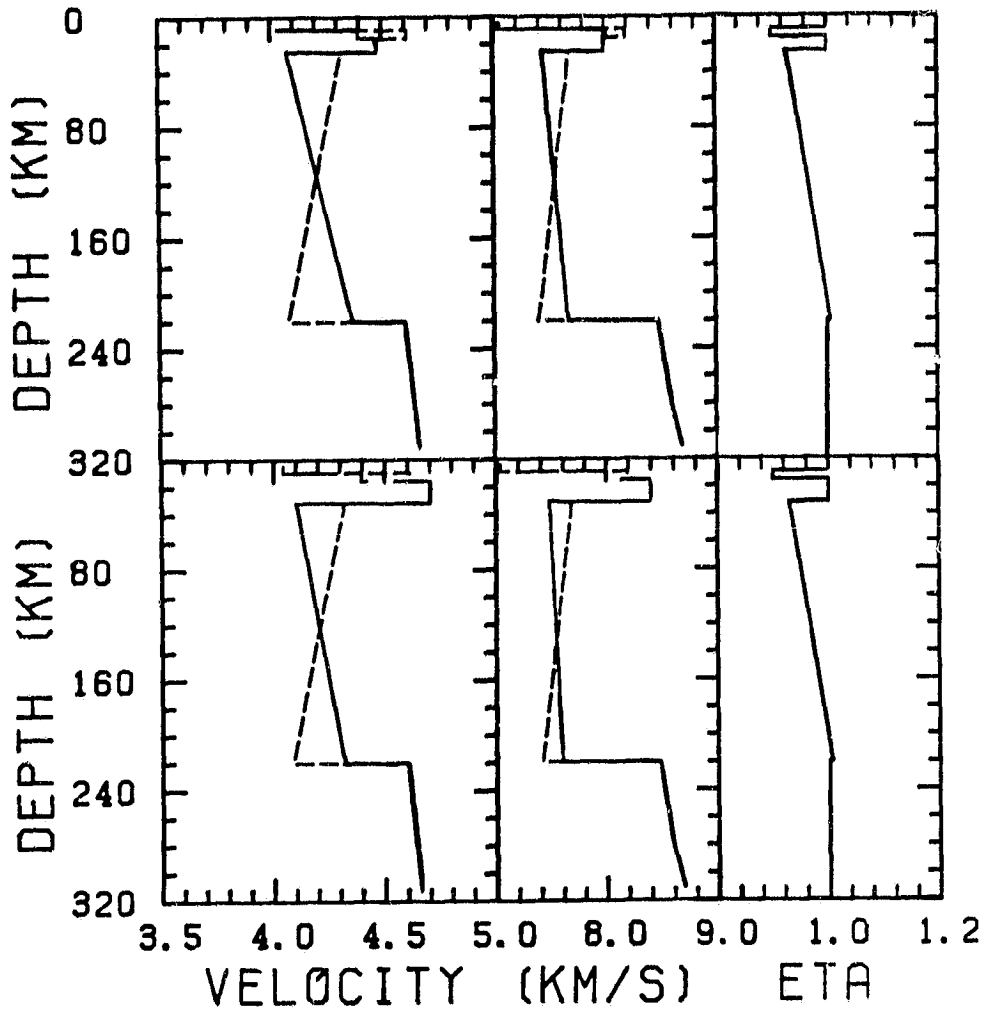

Fig. 19

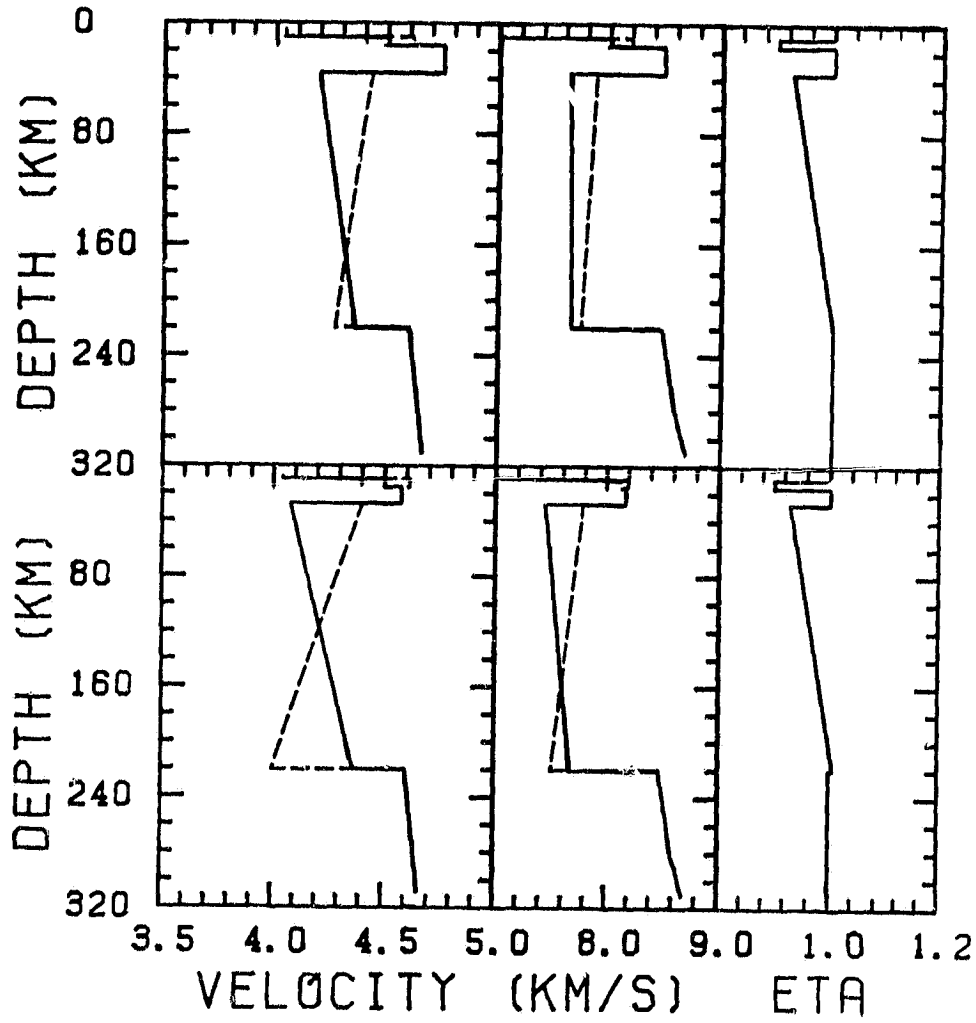

Fig. 20

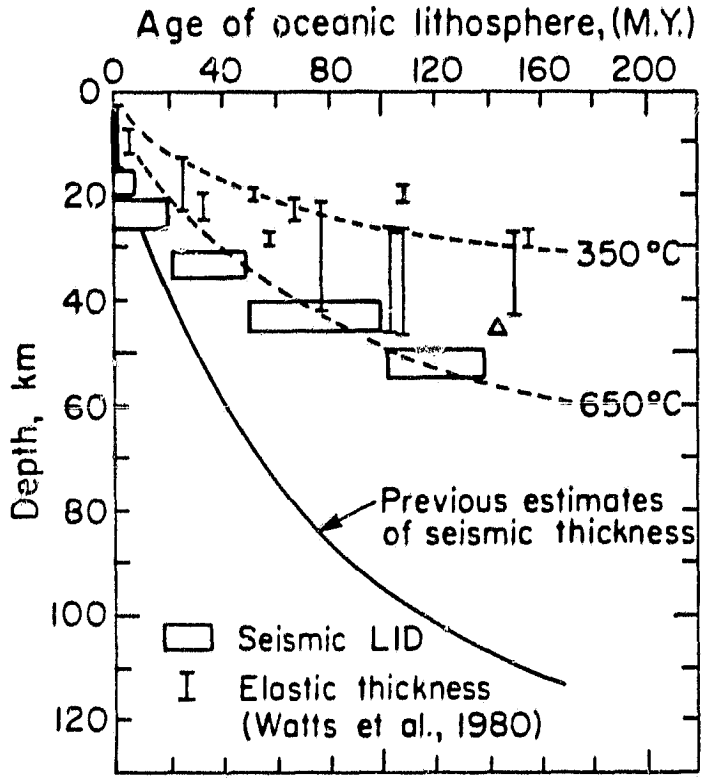

Fig. 21

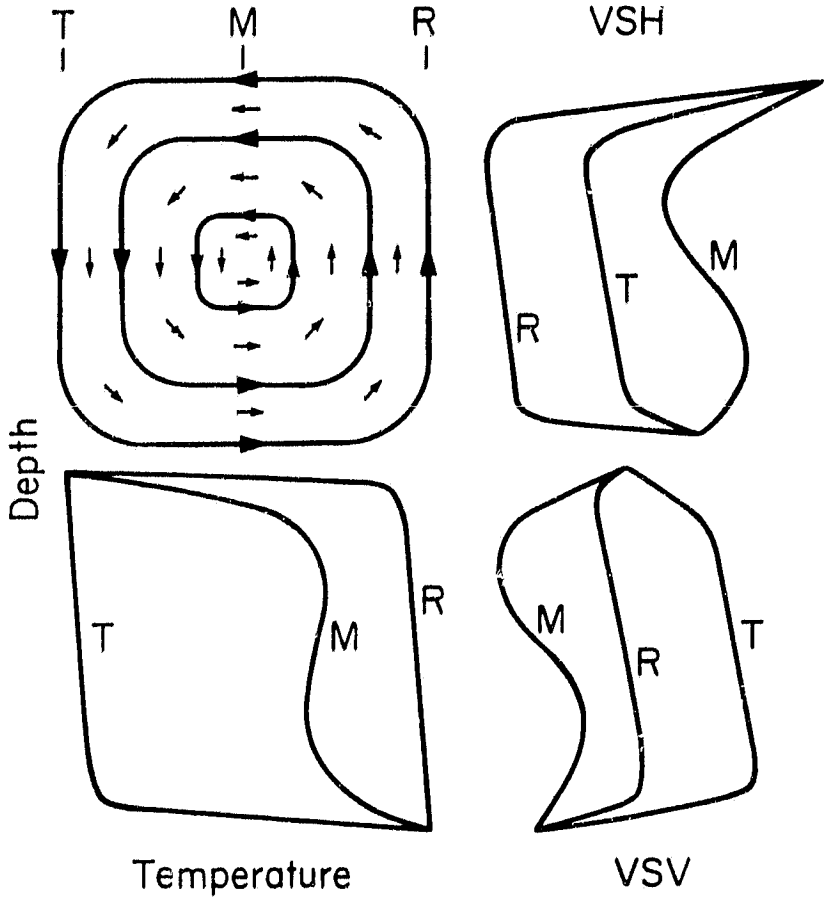

Fig. 22